Molecular Evolution of the Meiotic Recombination Pathway in Mammals

Investigations

Amy L. Dapper[1,2*] and Bret A. Payseur[1]

[1] Laboratory of Genetics, University of Wisconsin, Madison, WI 53706, USA

[2] Department of Biological Sciences, Mississippi State University, Mississippi State, MS 39762, USA

Running Title: Evolution of the Recombination Pathway

Keywords: pathway evolution, evolutionary rate, adaptive evolution, divergence, crossover

* Corresponding Author : Amy L. Dapper

Address: 295 E. Lee Blvd., P.O. Box GY, Mississippi State, MS 39762

Phone: (662) 325-7575

Email: dapper@biology.msstate.edu

Abstract

Meiotic recombination, the exchange of genetic material between homologous chromosomes during meiosis, is required for successful gametogenesis in most sexually reproducing species. Recombination is also a fundamental evolutionary force, influencing the fate of new mutations and determining the genomic scale over which selection shapes genetic variation. Species recombine at different rates, but the genetic basis of this evolution is poorly understood and the molecular evolution of most recombination genes remains uncharacterized. Using a phylogenetic comparative approach, we measure rates of evolution in 32 recombination pathway genes across 16 mammalian species, spanning primates, murids, and laurasithians. By analyzing a carefully-selected panel of genes involved in key components of recombination – spanning double strand break formation, strand invasion, the crossover/non-crossover decision, and resolution – we generate a comprehensive picture of the evolution of the recombination pathway in mammals. Recombination genes exhibit marked heterogeneity in the rate of protein evolution, both across and within genes. We report signatures of rapid evolution and positive selection that could underlie species differences in recombination rate. In particular, we highlight *TEX11* and associated genes involved in the synaptonemal complex and the early stages of the crossover/non-crossover decision as candidates for the evolution of recombination rate. We also reveal that genes involved in recombination exhibit strong correlations in evolutionary rate, including among genes known to physically interact.

Introduction

The reciprocal exchange of DNA between homologous chromosomes during meiosis – recombination – is required for successful gametogenesis in most species that reproduce sexually (Hassold and Hunt 2001). The rate of recombination is a major determinant of patterns of genetic diversity in populations, influencing the fate of new mutations (Hill and Robertson 1966), the efficacy of selection (Felsenstein 1974; Charlesworth *et al.* 1993; Comeron *et al.* 1999; Gonen *et al.* 2017), and several features of the genomic landscape (Begun and Aquadro 1992; Charlesworth *et al.* 1994; Duret and Arndt 2008).

Although recombination rate is often treated as a constant, this fundamental parameter evolves over time. Genomic regions ranging in size from short sequences to entire chromosomes vary in recombination rate – both within and between species (Burt and Bell 1987; Broman *et al.* 1998; Jeffreys *et al.* 2005; Coop and Przeworski 2007; Kong *et al.* 2010; Dumont *et al.* 2011; Smukowski and Noor 2011; Comeron *et al.* 2012; Segura *et al.* 2013; Dapper and Payseur 2017; Stapley *et al.* 2017).

Genome-wide association studies are beginning to reveal the genetic basis of differences in recombination rate within species. Individual recombination rates have been associated with variation in specific genes in populations of *Drosophila melanogaster* (Hunter *et al.* 2016), humans (Kong *et al.* 2008, 2014; Chowdhury *et al.* 2009; Fledel-Alon *et al.* 2011), domesticated cattle (Sandor *et al.* 2012; Ma *et al.* 2015; Kadri *et al.* 2016; Shen *et al.* 2018), domesticated sheep (Petit *et al.* 2017), Soay sheep (Johnston *et al.* 2016), and red deer (Johnston *et al.* 2018). Variants in several of these genes correlate with recombination rate in multiple species, including: *RNF212* (Kong *et al.* 2008; Chowdhury *et al.* 2009; Fledel-Alon *et al.* 2011; Sandor *et al.* 2012; Johnston *et al.* 2016; Kadri *et al.* 2016; Petit *et al.* 2017), *RNF212B* (Johnston *et al.* 2016, 2018; Kadri *et al.* 2016), *REC8* (Sandor *et al.* 2012; Johnston *et al.* 2016, 2018), *HEI10/CCNB1IP1* (Kong *et al.* 2014; Petit *et al.* 2017), *MSH4* (Kong *et al.* 2014; Ma *et al.* 2015; Kadri *et al.* 2016; Shen *et al.* 2018), *CPLX1* (Kong *et al.* 2014; Ma *et al.* 2015; Johnston *et al.* 2016; Shen *et al.* 2018) and *PRDM9* (Fledel-Alon *et al.* 2011; Sandor *et al.* 2012; Kong *et al.* 2014; Ma *et al.* 2015; Shen *et al.* 2018).

In contrast, the genetics of recombination rate variation among species remains poorly understood. Divergence at the di-cistronic gene *mei-217/mei-218* explains much of the disparity in genetic map length between *D. melanogaster* and *D. mauritiana* (Brand *et al.* 2018). *mei-217/mei-218* is the only gene known to confer a recombination rate difference between species, though quantitative trait loci that contribute to shifts in rate among subspecies of house mice have been identified (Murdoch *et al.* 2010; Dumont and Payseur 2011; Balcova *et al.* 2016).

One strategy for understanding how species diverge in recombination rate is to inspect patterns of molecular

evolution at genes involved in the recombination pathway. This approach incorporates knowledge of the molecular and cellular determinants of recombination and is motivated by successful examples. *mei-217/mei-218* was targeted for functional analysis based on its profile of rapid evolution between *D. melanogaster* and *D. mauritiana* (Brand *et al.* 2018). *PRDM9*, a protein that positions recombination hotspots in house mice and humans through histone methylation (Myers *et al.* 2010; Parvanov *et al.* 2010; Grey *et al.* 2011, Paigen2018; 2018), shows accelerated divergence across mammals (Oliver *et al.* 2009). The rapid evolution of *PRDM9* – which localizes to its zinc-finger DNA binding domain (Oliver *et al.* 2009) – appears to be driven by selective pressure to recognize new hotpot motifs as old ones are destroyed via biased gene conversion (Myers *et al.* 2010; Ubeda and Wilkins 2011; Lesecque *et al.* 2014; Latrille *et al.* 2017). Although these examples demonstrate the promise of signatures of molecular evolution for illuminating recombination rate differences between species, patterns of divergence have yet to be reported for most genes involved in meiotic recombination.

Mammals provide a useful system for dissecting the molecular evolution of the recombination pathway for several reasons. First, the evolution of recombination rate has been measured along the mammalian phylogeny (Dumont and Payseur 2008; Segura *et al.* 2013). Second, recombination rate variation has been associated with specific genes in mammalian populations (Kong *et al.* 2008, 2014; Chowdhury *et al.* 2009; Sandor *et al.* 2012; Ma *et al.* 2015; Johnston *et al.* 2016, 2018; Kadri *et al.* 2016; Petit *et al.* 2017; Shen *et al.* 2018). Third, laboratory mice have proven to be instrumental in the identification and functional characterization of recombination genes (Vries *et al.* 1999; Baudat *et al.* 2000; Romanienko and Camerini-Otero 2000; Yang *et al.* 2006; Ward *et al.* 2007; Schramm *et al.* 2011; Bisig *et al.* 2012; Bolcun-Filas and Schimenti 2012; La Salle *et al.* 2012; Kumar *et al.* 2015; Finsterbusch *et al.* 2016; Stanzione *et al.* 2016).

Work in mice indicates that the mammalian recombination pathway is roughly divided into five major steps, each of which is regulated by a handful of genes. The first step is the formation of hundreds of double strand breaks (DSBs) throughout the genome (Bergerat *et al.* 1997; Keeney *et al.* 1997; Baudat *et al.* 2000; Romanienko and Camerini-Otero 2000; Baudat and Massy 2007; Finsterbusch *et al.* 2016; Lange *et al.* 2016). After formation, DSBs are identified, processed, and paired with their corresponding location on the homologous chromosome through the processes of homology search and strand invasion (Keeney 2007; Cloud *et al.* 2012; Brown and Bishop 2014; Finsterbusch *et al.* 2016; Kobayashi *et al.* 2016; Oh *et al.* 2016; Xu *et al.* 2017). The pairing of homologous chromosomes is then stabilized by a proteinaceous structure referred to as the synaptonemal complex (SC) (Meuwissen *et al.* 1992; Schmekel and Daneholt 1995; Costa *et al.* 2005; Vries *et al.* 2005; Hamer *et al.* 2006; Yang *et al.* 2006; Schramm *et al.* 2011; Fraune *et al.* 2014; Hernández-Hernández *et al.* 2016). The SC also forms a substrate on which the eventual crossover events

will take place (Page and Hawley 2004; Hamer *et al.* 2008). It is at this point that a small subset of DSBs is designated to mature into crossovers, leaving the majority of DSBs to be resolved as non-crossovers (Snowden *et al.* 2004; Yang *et al.* 2008; Reynolds *et al.* 2013; Finsterbusch *et al.* 2016; Rao *et al.* 2017). Finally, this designation is followed, and each DSB is repaired as a crossover or a non-crossover (Baker *et al.* 1996; Edelmann *et al.* 1996; Lipkin *et al.* 2002; Rogacheva *et al.* 2014; Xu *et al.* 2017).

In this article, we examine the molecular evolution of 32 key recombination genes, evenly distributed across each major step in the recombination pathway, in 16 mammalian species spanning primates, murids, and laurasiatherians. Our results point to steps of the pathway most likely to contribute to differences in recombination rate between species.

Materials and Methods

Data Acquisition & Processing

We selected a focal panel of 32 recombination genes (See Table1). The panel was constructed to: (1) cover each major step in the recombination pathway as evenly as possible, (2) contain genes that have integral functions in each step, and (3) include genes that have been associated with inter-individual differences in recombination rate within mammalian populations. Reference sequences from 16 species of mammals for each gene were downloaded from both NCBI and Ensembl (Release-89)(Wheeler *et al.* 2006; Zerbino *et al.* 2017).

Alternative splicing is widespread and presents a challenge for molecular evolution studies (Pan *et al.* 2008; Barbosa-Morais *et al.* 2012). To focus our analyses on coding sequences that are transcribed during meiosis and to validate the computational annotations for each gene in each species, we used available testes expression datasets. We downloaded raw testes expression data for each species from NCBI Gene Expression Omnibus (GEO) (Table S1)(Barrett *et al.* 2012). We converted the SRA files into FASTQ files using SRAtoolkit (Leinonen *et al.* 2010). The reads were mapped to an indexed reference genome (Tables S2 and S3)(Bowtie2; Langmead and Salzberg 2012) using TopHat (Trapnell *et al.* 2009). The resulting bam files were sorted using Samtools (Li *et al.* 2009) and visualized using IGV 2.4.10 (Thorvaldsdóttir *et al.* 2013). We used this approach to: (1) identify the transcript expressed in testes, (2) check the reference transcript for errors, and (3) revise the reference transcript based upon the transcript data.

We compared expression data to annotations from both Ensembl and NCBI (Wheeler *et al.* 2006; Zerbino *et al.* 2017). When both transcripts were identical, we selected the NCBI transcript. The Ensembl transcript was used instead when: (1) the NCBI reference sequence was not available, (2) when none of the NCBI transcripts

matched the expression data, or (3) when there were sequence differences between the two transcripts and the Ensembl transcript was more parsimonious (i.e. had the fewest differences when compared to the rest of sequences in the alignment). The use of testes expression data was a key quality control step and the inclusion of species in this study was primarily determined by the availability of testes expression data.

Phylogenetic Comparative Approach

For each gene, we used phylogenetic analysis by maximum likelihood (PAML 4.8) to measure the rate of evolution across the mammalian phylogeny and to search for molecular signatures indicative of positive selection (Table 2) (Yang 1997, 2007). This approach requires a sequence alignment and a phylogenetic tree. For each gene, sequences were aligned using Translator X, a codon-based alignment tool, powered by MUSCLE v3.8.31 (Edgar 2004; Abascal *et al.* 2010). Each alignment was examined by hand and edited as necessary. We used a species tree that reflects current understanding of the phylogenetic relationships of the species included in our study (Figure 1)(Prasad *et al.* 2008; Perelman *et al.* 2011; Fan *et al.* 2013; Chen *et al.* 2017).

Due to the ambiguity in the relationship between laurasithians and the placement of tree shrews, we also inferred gene trees using MrBayes (Ronquist *et al.* 2012; Fan *et al.* 2013; Chen *et al.* 2017). To infer each gene tree, we selected the General Time Reversible (GTR) substitution model with gamma-distributed rate variation across sites and the Markov chain Monte Carlo (mcmc) sampling was run until the standard deviation frequency was less than 0.01 (Ronquist *et al.* 2012). We used this approach to account for effects of incomplete lineage sorting (ILS) (Pamilo and Nei 1988; Rosenberg 2002; Scornavacca and Galtier 2017). Using gene trees and using the consensus species tree produced highly similar results (Table S5).

For 19 genes, transcripts from all 16 species were used. For 11 genes in which the chimpanzee and bonobo sequences were identical, we excluded the bonobo sequence. For one gene in which the chimpanzee, bonobo and human sequences were all identical, we excluded the chimpanzee and bonobo sequences. In only two cases, a suitable reference sequence could not be identified for a given species (*RNF212B*: Rat; *TEX11*: Tree Shrew).

We estimated rates of synonymous and non-synonymous substitutions per site using the CODEML program in PAML4.8 (Yang 2007). This program considers multiple substitutions per site, different rates of transitions and transversions, and effects of codon usage (Yang 2007). Rates of substitution were computed for 6 different models of molecular evolution (Table 2). The fit of each model was compared using a likelihood ratio test. Reported substitution rates assume the best-fit model for each gene.

Identifying Signatures of Selection

To test for positive selection, we compared the fit of models including a class of sites with $\omega > 1$ to the fit of models in which all classes of sites have $\omega \leq 1$. Specifically, we report three comparisons: M1 vs. M2, M7 vs. M8, and M8 vs. M8a (Table 2). The first comparison, M1 vs. M2, compares a model with two classes of sites ($\omega < 1$, $\omega = 1$) to a model with a third class of sites where $\omega > 1$, indicative of positive selection (Yang 2007). More complex models (M7 & M8) were developed to consider variation in $\omega < 1$ among sites within genes by including 10 site classes drawn from a beta distribution ranging from 0 to 1 (Yang 2007). In this case, Model 8 includes one additional class of sites in which $\omega > 1$ (for a total of 11 site classes), allowing for the identification of signatures of positive selection (Yang 2007). In cases in which a large fraction of sites within a gene are evolving neutrally ($\omega = 1$), Model 8 will fit significantly better due to a very poor fit of Model 7 rather than a signature of positive selection. To avoid incorrectly identifying signatures of positive selection in this case, we also compared Model 8 to Model 8a, which contains a larger fraction of neutrally evolving sites than Model 7 (Swanson *et al.* 2003). We report the number of codons in each gene estimated to have $\omega > 1$ (Bayes-Empiricial-Bayes (BEB); $P > 0.95$).

Multinucleotide Mutations

Multi-nucleotide mutations (MNMs) occur when two mutations happen simultaneously in close proximity (Schrider *et al.* 2011; Besenbacher *et al.* 2016). MNMs violate the PAML assumption that the probability of two simultaneous mutations in the same codon is 0 (Yang 2007; Venkat *et al.* 2018). Recent work has shown that MNMs can lead to the false inference of positive selection when using branch-site tests in PAML (Venkat *et al.* 2018). Although we did not use branch-site tests, it is possible that MNMs contributed to some of the signatures of positive selection we observed. Although we could not directly identify MNMs in our dataset, we conducted an additional analysis to gauge the potential effects of MNMs on our results. We used PAML to reconstruct the ancestral sequence at each node in the phylogeny (Yang 2007). For the reconstruction, Model 8 was chosen because we specifically re-analyzed genes that showed evidence for positive selection when comparing Model 7 with Model 8. From the ancestrally reconstructed sequences, we identified any codons in which PAML inferred more than 1 substitution on a single branch (codons with multiple differences; CMDs). All identified CMDs were removed from the sequences in which they occurred. For example, if a CMD was identified in an external branch, that codon was replaced with '—' only in the sequence of that species. If a CMD was inferred on an internal branch, the codon was replaced with '—' in all species descended from that internal branch. For each gene that showed evidence of positive selection using the unedited sequences, we

also conducted PAML analyses using sequences from which all CMDs were removed.

Polymorphism & Divergence in the Primate Lineage

To further examine evidence for selection on recombination genes, we compared divergence between humans and macaque to polymorphism within humans in the recombination genes. Human polymorphism data was downloaded from ExAC database (Lek *et al.* 2016). The ExAC database spans 60,706 unrelated individuals sequenced as part of both disease-specific and population genetic studies (Lek *et al.* 2016). To avoid biases introduced by population structure, we restricted our analyses to the population with the largest representation in the database: European, non-Finnish, individuals (N = 33,370)(Lek *et al.* 2016). Polymorphism data for the correct transcript of *RNF212* (based upon expression data) was not available in the ExAC database; this gene was not included in this analysis.

We compared counts of non-synonymous and synonymous polymorphisms to counts of non-synonymous and synonymous substitutions using the McDonald-Kreitman test (McDonald and Kreitman 1991). The neutral expectation is that the ratio of non-synonymous to synonymous substitutions is equal to the ratio of non-synonymous to synonymous polymorphisms (McDonald and Kreitman 1991). Significant deviations provide evidence of natural selection. The neutrality index (NI) measures the direction and degree of departures from the neutral expectation (Charlesworth 1994). An NI < 1 indicates positive selection, and the fraction of adaptive amino acid substitutions can be estimated as 1 - NI (Charlesworth 1994; Fay *et al.* 2001; Smith and Eyre-Walker 2002). We also measure the direction of selection (DoS) for each gene, an additional statistic that estimates the direction and degree of departures from the neutral expectation and has been shown to be less biased than NI under certain conditions (Stoletzki and Eyre-Walker 2010). A positive DoS is consistent with positive selection; a negative DoS indicated purifying selection (Stoletzki and Eyre-Walker 2010). Additionally, we estimated pairwise divergence (ω) between human and macaque using the *yn00* package in PAML (Table 5 and Table S4) (Yang 2007).

Identifying Evolutionary Patterns

To identify evolutionary patterns among recombination genes, we compared the rate of evolution and the proportion of genes experiencing positive selection among groups of interest. We asked: (1) Do genes that function in different steps of the pathway exhibit different rates of evolution? (2) Do genes that function post-synapsis evolve more rapidly than genes that function pre-synapsis? and (3) Do genes associated with variation in recombination rate (within species) diverge more rapidly between species? All statistical analyses

were performed in R (R Core Team 2015).

To determine whether recombination genes co-evolve, we computed the evolutionary rate covariation (ERC) metric: the correlation coefficient between branch-specific rates among pairs of proteins (Clark *et al.* 2012). ERC is frequently elevated among interacting proteins (Pazos and Valencia 2001; Hakes *et al.* 2007; Clark *et al.* 2009) and is assumed to result from: (1) concordance in fluctuating evolutionary pressures, (2) parallel evolution of expression level, and/or (3) compensatory changes between co-evolving genes (Clark *et al.* 2012, 2013; Priedigkeit *et al.* 2015). We used a publicly available ERC dataset (https://csb.pitt.edu/erc_analysis/index.php) to compare the median ERC-value among a subset of the focal recombination genes ($N = 25$) to other genes in the genome, as described in Priedigkeit et al. (2015).

To control for an observed elevation in ERC among recombination genes and test for relationships between specific groups, we also conducted an ERC analysis that was restricted to the focal set of 32 recombination genes. Branch lengths were calculated using the *aaML* package in PAML (Yang 2007) and pairwise ERC values were calculated following the methods of Clark et al. (2012). Using this approach, we specifically compared the ERC values among three of the most rapidly evolving recombination genes (*TEX11*, *SHOC1*, and *SYCP2*) to the other recombination genes.

Data Availability

Sources and accession numbers for all publicly available sequence data used in this study can be found in Supplemental Tables S1-S3. All data, sequence alignments, and code necessary to replicate this study can be found in the following publicly available GitHub Repository (https://github.com/adapper/Evo_RecGenes_MS).

Results

Recombination genes evolve at different rates in mammals

We observed substantial heterogeneity in the rate of evolution of recombination genes, spanning a range of 0.0268 – 0.8483 (mean $\omega = 0.3275$, SD = 0.1971, median = 0.3095) (Figure 2A, Figure 3, Table 3). Four genes exhibit particularly rapid evolution compared to other recombination genes, with evolutionary rates greater than 1 SD above the mean (*IHO1*, *SHOC1*, *SYCP2*, *TEX11*). At the other end of the spectrum, five genes have evolutionary rates more than 1 SD below the mean and are highly conserved across the mammalian phylogeny (*BRCC3*, *DMC1*, *HEI10*, *RAD50*, *RAD51*). In comparisons between human and macaque, six genes have evolutionary rates more than 1 SD above the mean (*CNTD1*, *IHO1*, *MEI4*, *RAD21L*, *SHOC1*,

TEX11) and six genes have evolutionary rates more than 1 SD below the mean (*DMC1*, *HORMAD1*, *MLH1*, *MRE11*, *RAD50*, *RAD51*). The genes that show the most rapid and most conserved rates of divergence between humans and macaques are mostly the same genes that show extreme evolutionary rates across the mammalian phylogeny. Notable exceptions include *MEI4* ($\omega_{\text{mammals}} = 0.4332$, $\omega_{\text{human-macaque}} = 0.7252$), *CNTD1* ($\omega_{\text{mammals}} = 0.2496$, $\omega_{\text{human-macaque}} = 0.6803$), *HEI10* ($\omega_{\text{mammals}} = 0.1226$, $\omega_{\text{human-macaque}} = 0.3235$), and *HORMAD1* ($\omega_{\text{mammals}} = 0.3036$, $\omega_{\text{human-macaque}} = 0.0901$. In general, there is very high concordance between evolutionary rate across mammals and pairwise divergence between humans and macaques (mean $\omega = 0.3301$, SD = 0.2370, median = 0.30925)(Spearman's $\rho = 0.833774$, $p = 3.11\text{e-}9$)(Figure 2B, Table 4). It should be noted that these two measures are not independent because divergence between human and macaque sequences was incorporated in the phylogenetic analysis across mammals.

Recombination genes evolve faster than other genes in primates

Gradnigo et al. (2016) measured the rate of divergence between human and macaque for 3,606 genes throughout the genome. We used this dataset to ask whether the rate of evolution of recombination genes as a group is different than expected from the genome-wide distribution. Mean rates for sets of 32 ω values randomly sampled from the 3,606-gene list rarely exceeded the mean rate for recombination genes ($p = 0.0075$, 10,000 random draws) (Figure 4), suggesting that recombination genes evolve faster on average, at least between human and macaque.

Recombination genes display signatures of positive selection across mammals

Comparing polymorphism within humans to divergence between human and macaque revealed that 17 out of 31 genes depart from neutral predictions in the form of significant McDonald-Kreitman tests (Fisher's Exact Test, $p < 0.05$; Table 5). These seventeen genes harbor an excess of non-synonymous polymorphisms (Table 5). This pattern suggests the presence of weakly deleterious mutations at recombination genes in human populations. Contrary to predictions under this model, however, we detected no significant differences in allele frequency between non-synonymous and synonymous polymorphism (Wilcoxon rank sum test; $p > 0.05$**). None of the recombination genes we surveyed displays a significant excess of non-synonymous substitutions, the expected signature of positive selection. Only one gene (*TEX11*) has a higher ratio of non-synonymous to synonymous substitutions than non-synonymous to synonymous polymorphisms ($NI = 0.7879$; $DoS = 0.0534$)(Table 5).

In contrast to conventional McDonald-Kreitman tests, phylogenetic comparative methods enable the identifi-

cation of signatures of selection acting on a subset of sites within a gene over long evolutionary timescales. We identified signatures of positive selection in 11 of 32 (34.3%) recombination genes using site models in *CODEML*: *IHO1*, *MSH4*, *MRE11*, *NBS1*, *RAD21L*, *REC8*, *RNF212*, *SHOC1*, *SYCP1*, *SYCP2*, and *TEX11* (Table 2). For each of these genes, models that include a fraction of sites where the rate of non-synonymous substitutions is estimated to be greater than the rate of synonymous substitutions ($\omega > 1$, Model 8) fit better than models that did not include such a class of sites (Model 7, 8a). To mitigate the potential for multi-nucleotide mutations to produce false signatures of positive selection, we re-analyzed this subset of genes after removing any codons inferred to have accumulated multiple changes on a single branch (CMDs). After removing all CMDs, 1 gene (*TEX11*) retained a significant signature of positive selection (Table 5).

Recombination genes associated with inter-individual differences do not diverge more rapidly between species

Recombination genes previously associated with inter-individual differences in recombination rate within species do not evolve significantly faster between species of mammals (average $\omega = 0.3943$ vs. average $\omega = 0.2925$, respectively; $p = 0.2381$, Mann-Whitney U Test), though the difference in evolutionary rates between these two classes of genes is greater when considering only divergence between humans and macaques (average $\omega = 0.4181$ vs. average $\omega = 0.2839$, respectively; $p = 0.08816$, Mann-Whitney U Test). Likewise, the proportion of recombination genes that exhibit signatures of positive selection is not significantly higher among genes that have been associated with inter-individual differences (5/11 vs. 6/21; $p = 0.4424$, Fisher's Exact Test).

Recombination gene evolution does not depend strongly on position in the pathway

Comparisons among groups of genes assigned to six major steps in the recombination pathway yielded no significant differences in evolutionary rate (mammals: $p = 0.1422$, Kruskal-Wallis Test; human vs. macaque: $p = 0.2682$, Kruskal-Wallis Test)(Figure 6). Similarly, genes acting before and after synapsis show similar evolutionary rates across mammals (average $\omega_{\text{before}} = 0.2723$ vs. $\omega_{\text{after}} = 0.3762$, $p = 0.1425$, Mann-Whitney U Test). Post-synapsis genes show modest evidence of evolving faster than pre-synapsis genes in comparisons between human and macaque (average $\omega_{\text{before}} = 0.2514$ vs. $\omega_{\text{after}} = 0.3994$, $p = 0.05827$, Mann-Whitney U Test).

Evolutionary rates are correlated among recombination genes

We used a publicly available database (https://csb.pitt.edu/erc_analysis/index.php) to measure correlations in evolutionary rate among pairs of recombination genes across mammals. Recombination genes show levels of evolutionary rate covariation (mean ERC = 0.134) that are significantly higher than the genome-wide distribution of gene pairs (permutation $p = 0.000358$).

Motivated by the findings that *TEX11*, *SYCP2*, and *SHOC1* are three of the most rapidly evolving recombination genes among mammals (Table 3) and that *TEX11* has direct protein-to-protein interactions with both *SHOC1* and *SYCP2* (Yang *et al.* 2008; Guiraldelli *et al.* 2018), we focused on rate correlations between these genes. *TEX11*, *SYCP2*, and *SHOC1* show significantly higher rate correlations (mean ERC = 0.42369) than randomly sampled subsets of recombination genes (permutation $p = 0.025$).

Discussion

Species of mammals recombine at different rates (Burt and Bell 1987 ; Dumont and Payseur 2008; Smukowski and Noor 2011; Segura *et al.* 2013; Stapley *et al.* 2017), but the genetic changes responsible for this evolution remain unknown. Patterns of molecular divergence we discovered point to genes and steps in the pathway that are good candidates for the evolution of recombination rate.

Genes involved in meiotic recombination vary substantially in evolutionary rate. Genes that are highly conserved across the mammalian phylogeny (*BRCC3*, *DMC1*, *HEI10*, *RAD50*, and *RAD51*) mostly function in the detection and processing of DSB breaks (except *HEI10*; Dong *et al.* 2003; Hopfner 2005; Keeney 2007; Ward *et al.* 2007; Cloud *et al.* 2012; Qiao *et al.* 2014; Kobayashi *et al.* 2016), suggesting that these processes are not primary drivers of recombination rate evolution in mammals.

Four genes exhibit especially rapid evolution across the mammalian phylogeny (compared to other recombination genes): *IHO1*, *SHOC1*, *SYCP2*, and *TEX11*. Three of these genes are known to interact. *TEX11* binds to the synaptonemal complex, including *SYCP2*, and recruits proteins, including *SHOC1*, that regulate the first step of the crossover vs. non-crossover decision (Yang *et al.* 2008; Guiraldelli *et al.* 2018). *IHO1* recruits and activates *SPO11*, a topoisomerase-like protein that generates DSBs (Stanzione *et al.* 2016). Eleven of the 32 recombination genes we examined display signatures of positive selection across the mammalian phylogeny. These genes are predominantly found in two steps of the pathway - formation of the synaptonemal complex (*REC8*, *RAD21l*, *SYCP1*, and *SYCP2*; Parisi *et al.* 1999; Vries *et al.* 2005; Yang *et al.* 2006; Lee and Hirano 2011) and regulation of the first steps of the crossover vs. non-crossover decision (*TEX11*, *SHOC1*, *RNF212*,

and *MSH4*; Snowden *et al.* 2004; Yang *et al.* 2008; Qiao *et al.* 2014; Guiraldelli *et al.* 2018) - raising the possibility that adaptive evolution of these processes caused divergence in recombination rate among species. Five of these genes have been associated with inter-individual variation in recombination rate within species: *RAD21l* (Kong *et al.* 2014); *REC8* (Sandor *et al.* 2012; Johnston *et al.* 2016, 2018); *MSH4* (Kong *et al.* 2014; Ma *et al.* 2015; Kadri *et al.* 2016; Shen *et al.* 2018); *RNF212* (Kong *et al.* 2008; Chowdhury *et al.* 2009; Fledel-Alon *et al.* 2011; Sandor *et al.* 2012; Johnston *et al.* 2016; Kadri *et al.* 2016; Petit *et al.* 2017); and *TEX11* (Murdoch *et al.* 2010).

Our results highlight an evolutionary contrast between mammals and Drosophila. *MCMDC2*, the mammalian homolog of the *mei-217*/*mei-218* gene that evolves rapidly and adaptively in Drosophila (Brand *et al.* 2018), exhibits below average rates of evolution and no evidence of positive selection in mammals. These two homologs occupy different positions in the recombination pathway. In Drosophila, *mei-218* has evolved to replace the function of the missing *MSH4* and *MSH5* (Kohl *et al.* 2012; Finsterbusch *et al.* 2016). This shift in both evolutionary rate and pathway function suggests that functional homology is a better predictor of evolutionary rate than sequence homology for this recombination gene.

Deeper consideration of the recombination gene that shows the strongest evidence for positive selection, *TEX11*, provides additional clues about the genesis of recombination differences among mammals. Fourteen amino acid residues in *TEX11* exhibit patterns consistent with adaptive evolution (BEB, $P > 0.95$). In contrast to *MSH4* or *PRDM9* – where targets of selection localize to certain protein domains (Oliver *et al.* 2009; Thomas *et al.* 2009; Grey *et al.* 2011) – the *TEX11* residues of interest are distributed across the length of the gene. This pattern matches aspects of *TEX11* protein function. The gene encompasses three large, ubiquitous protein interaction (TRP) domains (Guiraldelli *et al.* (2018)). Most of the residues with signatures of selection localize to two of the large TRP domains, one of which is known to bind to *SHOC1* (Guiraldelli *et al.* 2018).

If mammals have experienced directional selection to increase crossover number (Segura *et al.* 2013), a key role for *TEX11* suggests that divergence in this trait reflects genetic changes acting early during the crossover/non-crossover decision. Alternatively, the positioning of *TEX11* at this stage in the pathway could suggest that selection favored a consistent recombination rate across the mammalian phylogeny. In this case, the signature of positive selection in *TEX11* could be driven by its role in maintaining crossover homeostasis despite the accumulation of changes in other genes in the pathway. The correlation in evolutionary rates between *TEX11*, *SYCP2*, and *SHOC1* can support either scenario (Clark *et al.* 2012, 2013). Either all three genes experience concordant selection pressures due to their similar functions in the recombination pathway or the correlation in evolutionary rate is driven by compensatory changes in *TEX11*. Notably, sequence

variation in *TEX11* has been associated with substantial difference in recombination rate in mice and in humans (Murdoch *et al.* 2010; Yang *et al.* 2015).

Genes in the recombination pathway reveal additional evolutionary patterns when considered as a group. Recombination genes tend to evolve faster than other genes, at least based on comparisons between human and macaque. Several factors could generate this pattern. First, the central role of recombination genes in reproduction could accelerate their divergence. The rapid evolution of reproductive genes is usually attributed to post-copulatory sexual selection or relaxed selection (from sex-specific expression and low female re-mating rates) (Swanson and Vacquier 2002; Dapper and Wade 2016). However, recombination occurs prior to copulation in mammals, and recombination genes are typically expressed in both sexes, two observations that argue against these explanations for elevated divergence. Second, the restriction of expression of some recombination genes to meiotic cells could reduce the pleiotropic consequences of amino acid substitutions (Duret and Mouchiroud 1999; Liao *et al.* 2006). A third possibility is that recombination itself is frequently subject to positive selection, driving divergence at the underlying genes (Dapper and Payseur 2017; Ritz *et al.* 2017).

Recombination genes previously associated with intra-specific variation in the genome-wide recombination rate evolve at similar rates to recombination genes lacking such an association. Genes responsible for species differences in recombination rate could be subject to strong directional selection within populations, reducing their contributions to intra-specific variation. Alternatively, genes that confer within-species rate variation could be targets of diversifying or antagonistic selection, limiting their divergence between species. For example, variants of *RNF212*, a gene associated with intra-specific variation in recombination rate in several mammalian species, have contrasting effects in women and men (Kong *et al.* 2008).

The structure of genetic pathways is expected to influence evolutionary trajectories (Rausher *et al.* 1999; Lu and Rausher 2003). Matching this prediction, recombination genes show relatively high rate correlations compared to other sets of genes. Nevertheless, our results suggest that the selection pressures targeting a gene are not easily deduced from its position in the recombination pathway. Perhaps rate variation among domains within proteins masks a clearer effect of pathway position. For example, the signal of adaptive evolution in *PRDM9* is restricted to the zinc finger residues, with much of the gene sequence being conserved between species (Oliver *et al.* 2009; Thomas *et al.* 2009). Rate heterogeneity between genes within steps of the recombination pathway motivates a more thorough investigation of functional domains in genes of interest.

Within-gene variation in evolutionary rate might explain another apparent discrepancy in our results.

Despite evidence for positive selection across the mammalian phylogeny at many genes, comparisons of polymorphism and divergence yielded no significant signatures of adaptive evolution between human and macaque. Instead, many recombination genes display an excess of non-synonymous polymorphisms, consistent with an accumulation of weakly deleterious mutations within humans. However, this approach searches for patterns of selection at the level of the entire gene, whereas positive selection can target certain domains. For example, *MSH4* exhibits evidence for adaptive evolution (though with a lower than average evolutionary rate) along the mammalian phylogeny and shows an excess of non-synonymous polymorphisms within humans. These two seemingly disparate results are unified by the observation that all 6 codons in *MSH4* with significant signatures of positive selection (BEB, $P > 0.95$) are highly localized in the first 100 bp of the gene, in a putative DNA binding domain (Rakshambikai *et al.* 2013; Piovesan *et al.* 2017).

One cost of the increased sensitivity of PAML is an inflation of the false-positive rate in the presence of multi-nucleotide substitutions (Venkat *et al.* 2018). It was not possible to directly identify MNMs in our dataset, so we chose the highly conservative approach of removing all codons inferred to have accumulated multiple mutations on a single branch in the phylogeny. Codons removed using this approach could be MNMs, but they also likely include codons that either have accumulated sequential mutations along the long branches in the mammalian phylogeny or are neither MNMs nor CMDs, due to uncertainty in the inference of ancestral sequences. Despite the conservative nature of this approach, we still found a signature of positive selection in *TEX11*, even when all putative CMDs were removed. Nevertheless, the conservative nature of the filter makes it difficult to draw conclusions about the robustness of signals of selection in the other recombination genes.

Another caveat concerns the interpretation of our findings. Although we would prioritize rapidly evolving genes with evidence of adaptive evolution as candidates, evolution of the recombination rate between species could be caused by only a few amino acid substitutions (especially along particular mammalian lineages) or by regulatory changes located outside protein-coding regions. We hope our results will motivate genetic dissection of between-species differences in recombination rate through functional evaluation of the candidate genes we identified, especially *TEX11* and associated gene involved in the synaptonemal complex and early stages of the crossover/non-crossover decision.

Acknowledgements

We thank Nathan Clark for assistance with evolutionary covariation rate analyses and Francesca Cole for advice on selection of recombination genes. A.L.D. was supported by NHGRI Training Grant to the Genomic Sciences Training Program 5T32HG002760. B.A.P. was supported by NIH grant NIH grant R01 GM120051.

Table 1 : List of 32 genes surveyed, organized by step in the recombination pathway. Genes in bold have been associated with inter-individual differences in recombination rate in at least one species of mammals.

Pathway Step	**Genes**
DSB Formation	*HORMAD1, IHO1, MEI4, SPO11,* ***REC114***
DSB Processing	*BRCC3, HORMAD2, MRE11, NBS1, RAD50*
Strand Invasion	*DMC1, MEIOB, MCMDC2, SPATA22, RAD51*
Homologous Pairing	*SYCP1, SYCP2,* ***RAD21L***, ***REC8***, *TEX12*
CO vs. NCO Decision	***MSH4***, ***MSH5***, ***RNF212***, ***RNF212B***, ***TEX11***, *SHOC1*
Resolution	*CNTD1,* ***HEI10***, ***MER3***, *MLH1,* ***MLH3***, *MUS81*

Table 2: Six PAML site models used to measure evolutionary rate and test for positive selection. Models varied in the number of ω classes, the range of ω for each of these classes, and whether a class of sites subject to positive selection was included.

Model	**# Site Classes**	**ω Range**	**Pos. Selection?**
0	1	<1	No
1	2	<1, =1	No
2	3	<1, =1, >1	Yes
7	10	0-1	No
8	11	0-1, >1	Yes
8a	6	0-1, =1	No

Figure 1: Species tree assumed in analyses of molecular evolution.

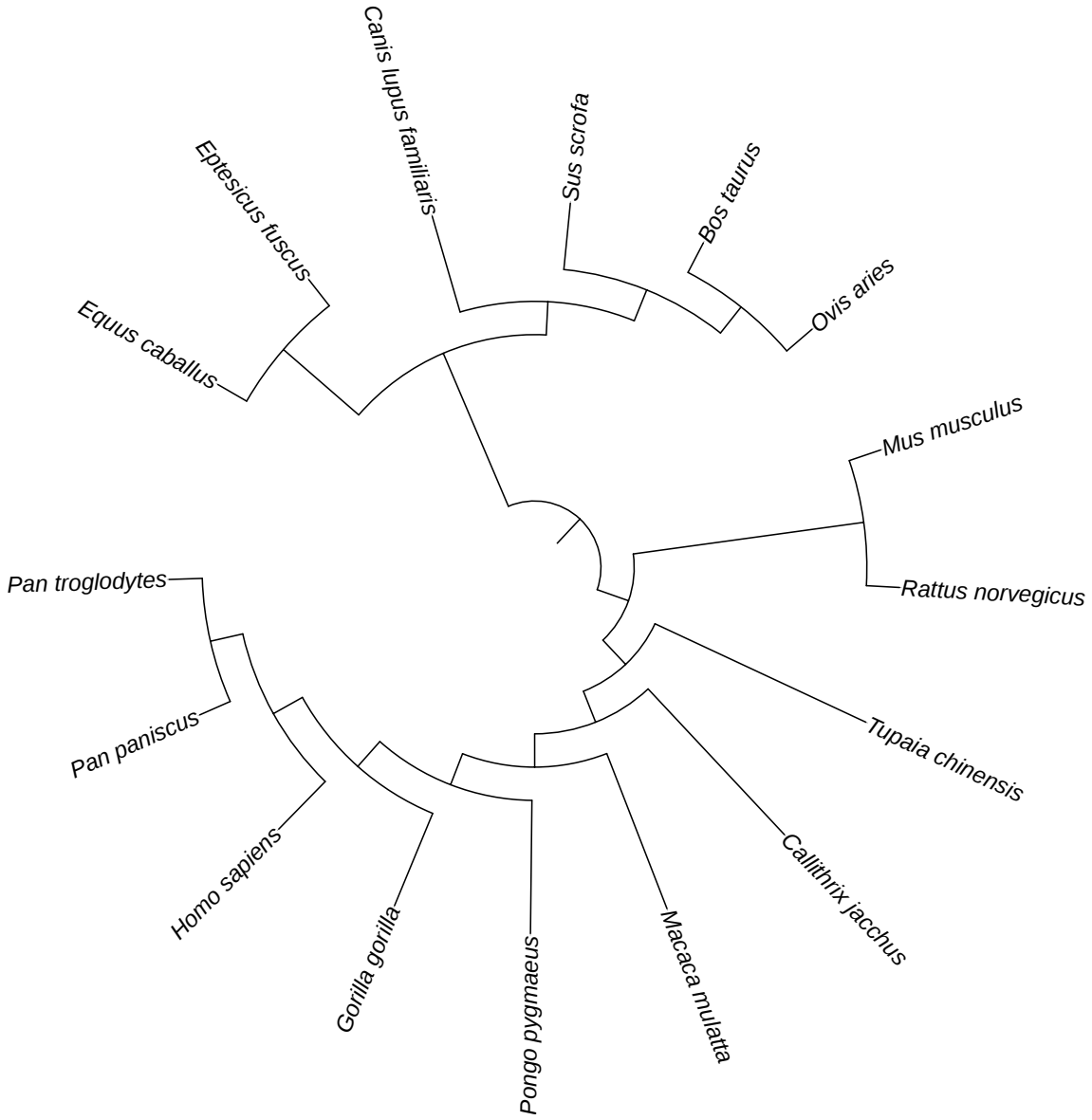

Figure 2:Distribution of ω for 32 recombination genes. Bar shows the mean +/- 1 standard deviation. (A) Divergence estimated across the mammalian phylogeny. (B) Pairwise divergence between human and macaque.

(A)

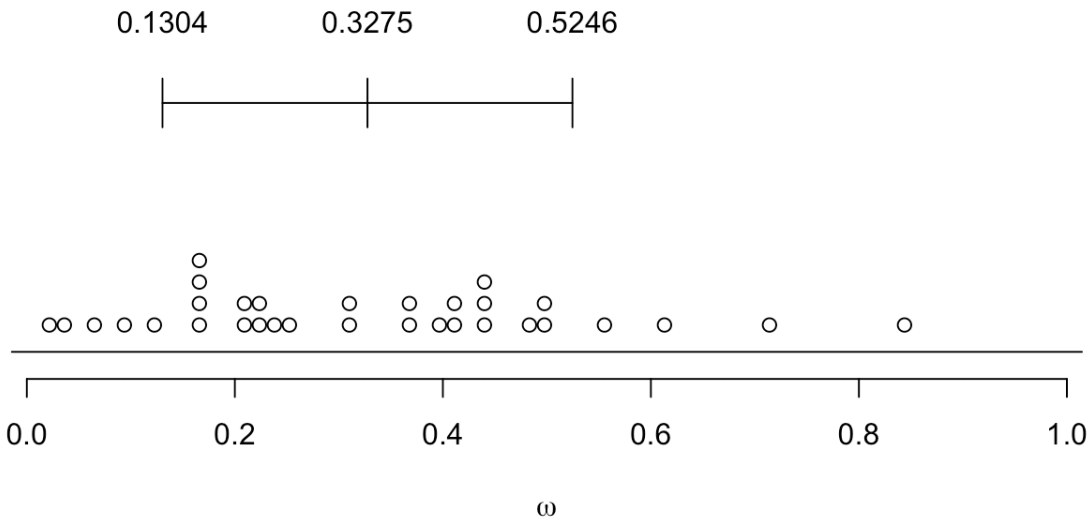

(B)

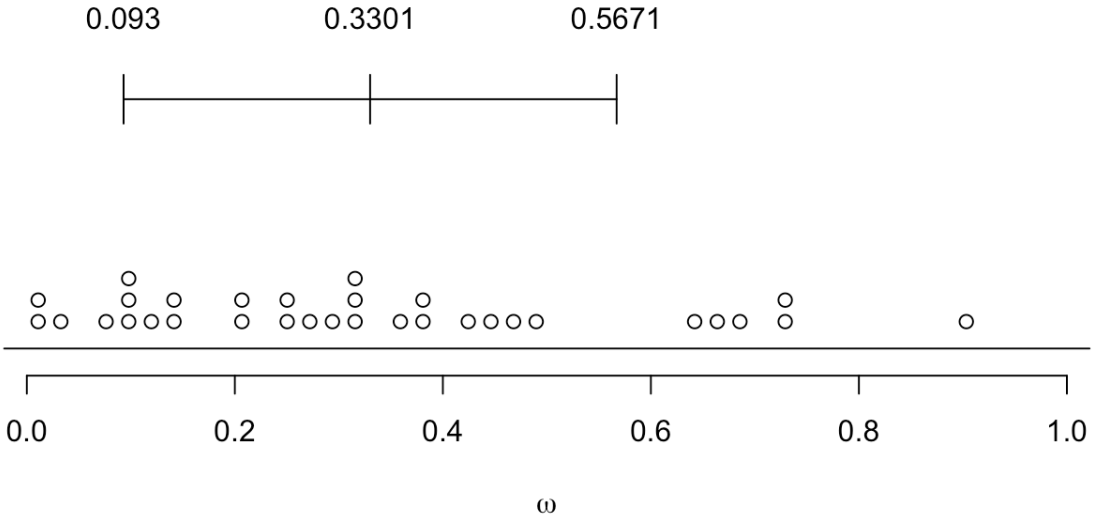

Figure 3: Evolutionary rate of key recombination genes in the context of the recombination pathway. The color of each gene represents its evolutionary rate relative to the average for recombination genes ($\omega = 0.3275$): more rapidly evolving genes are depicted in darker shades of red and more conserved genes are depicted in darker shades of blue. Genes that exhibit a signature of positive selection are in bold.

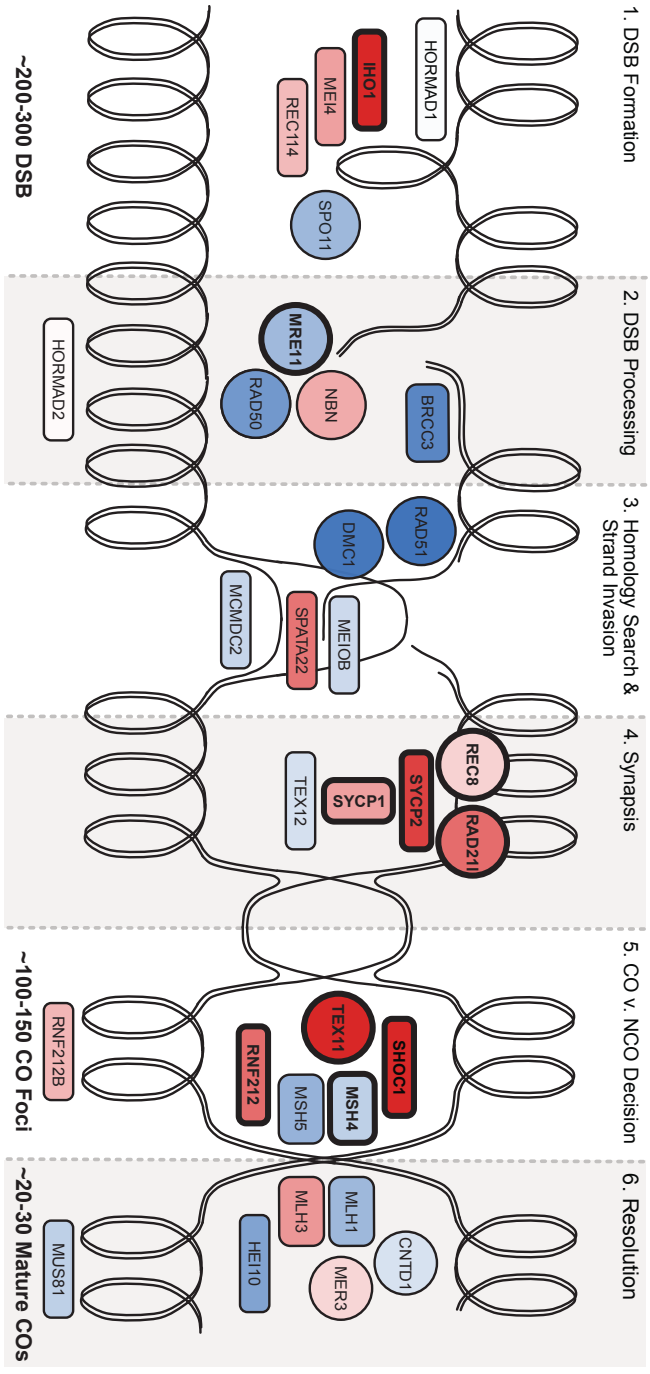

Figure 4: Distribution of average divergence (ω) between human and macaque of 10,000 gene sets randomly drawn from the entire genome. Average ω among these random draws was observed to be equal to or greater than that observed among recombination genes less than 1% of the time ($p = 0.0075$).

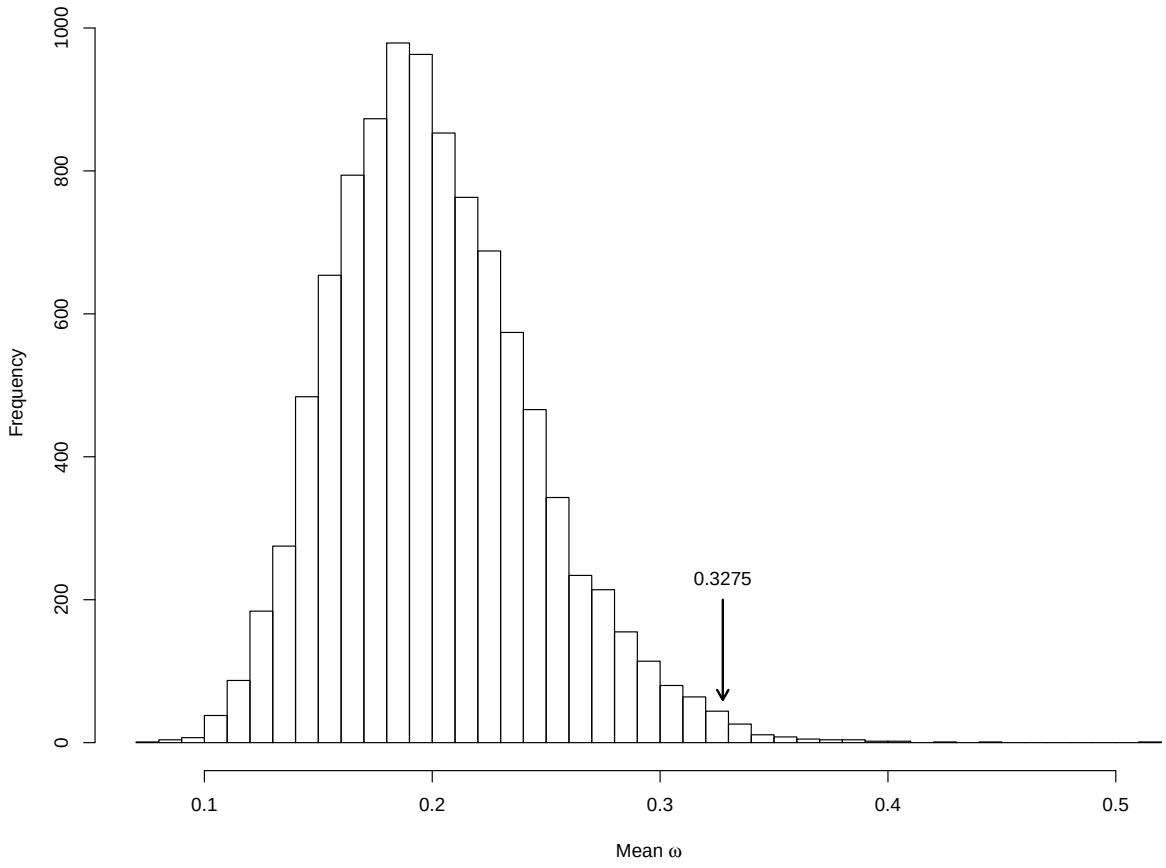

Figure 5: High concordance in evolutionary rate computed across mammals and between humans and macaque. The best-fit regression line is shown in red and the 1:1 line is shown as a dashed line.

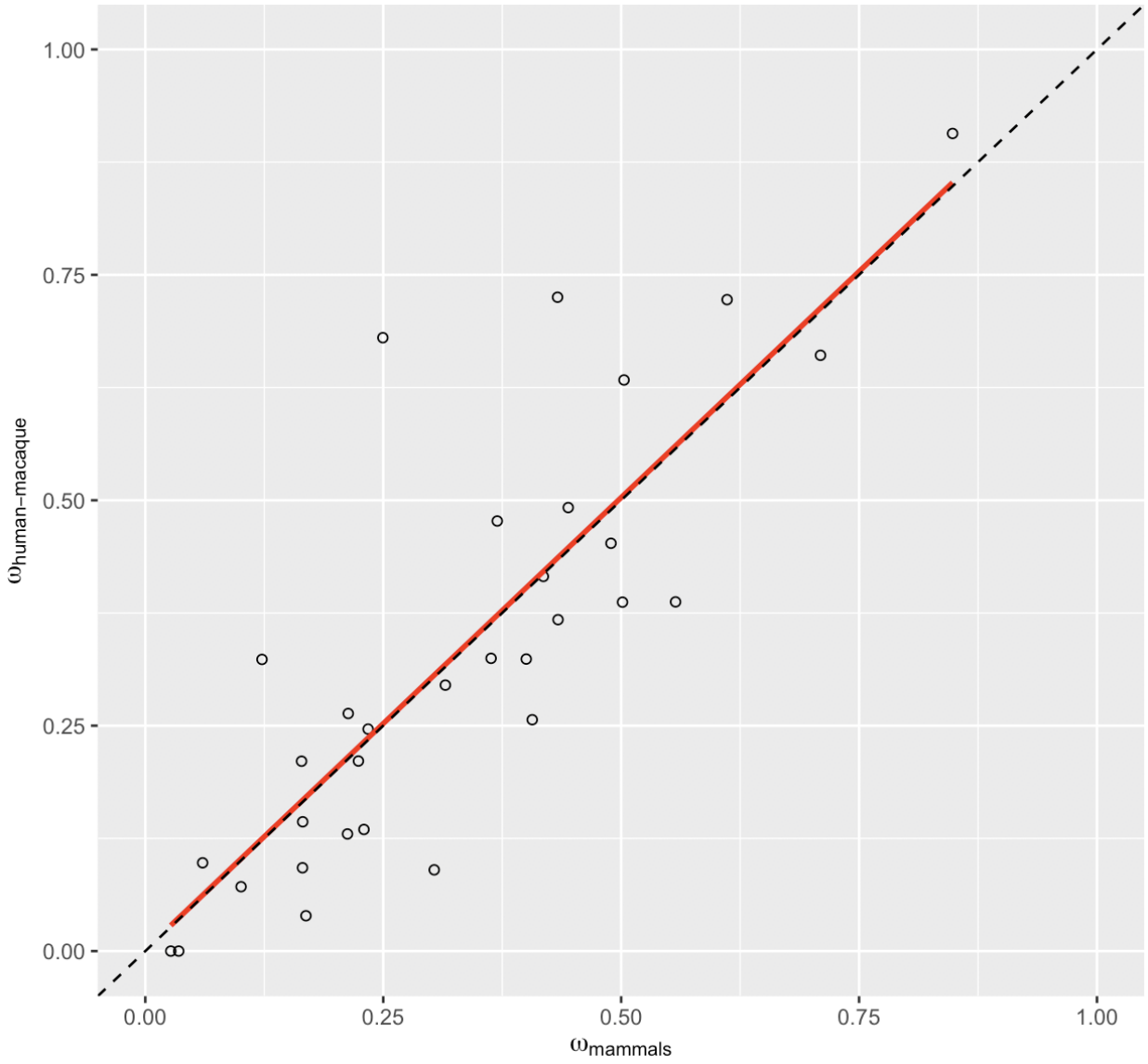

Figure 6: Boxplot of ω by step in recombination pathway.

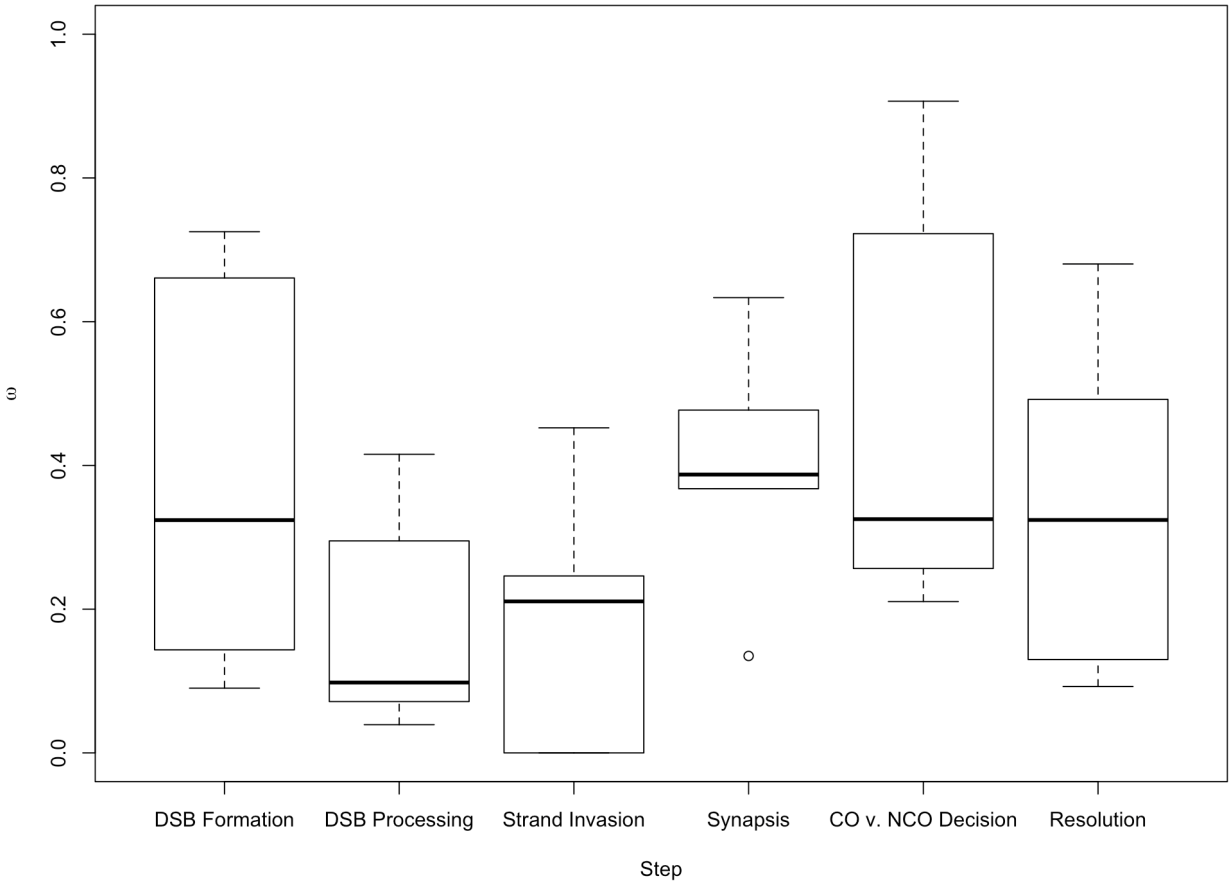

Table 3: Evolutionary rates and tests for positive selection across mammals at 32 recombination genes. Genes are organized by step in the pathway, as labeled in Figure 3.

Gene	***bp***	***N***	ω	***M***	***M1-M2***	***p-value***	***M7-M8***	***p-value***	***M8a-M8***	***p-value***	***BEB***
A)											
HORMAD1	1212	16	0.3036	7	0	*1.000*	1.795	*0.4076*	—	—	0
MEI4	1170	16	0.4332	7	0	*1.000*	0.005	*0.9976*	—	—	0
REC114	870	15	0.4003	7	0	*1.000*	5.384	*0.0677*	—	—	0
IHO1	1824	16	0.7095	**8**	13.061	***0.0015***	17.571	***0.0002***	14.527	***0.0001***	**1**
SPO11	1188	15	0.1654	7	0	*1.000*	4.648	*0.0980*	—	—	0
B)											
HORMAD2	981	15	0.3153	7	0	*1.000*	3.650	*0.1612*	—	—	0
MRE11	2136	16	0.1688	**8**	0.363	*0.8342*	11.931	***0.0026***	4.706	***0.0301***	0
NBS1	2289	15	0.4183	**8**	0	*1.000*	12.763	***0.0017***	4.087	***0.0432***	0
RAD50	3936	16	0.1006	7	0	*1.000*	0.301	*0.8605*	—	—-	0
BRCC3	954	15	0.0602	7	0	*1.000*	0.250	*0.8826*	—	—	0
C)											
DMC1	1020	15	0.0351	1	0.488	*0.7835*	5.000	*0.0821*	—	—	**1**
RAD51	1017	16	0.0268	7	0	*1.000*	0	*1.000*	—	—	0
SPATA22	1101	16	0.4893	7	0	*1.000*	0.429	*0.8070*	—	—	0
MEIOB	1425	16	0.2341	7	0	*1.000*	0.665	*0.7172*	—	—	0
MCMDC2	2052	16	0.2239	7	0	*1.000*	0.628	*0.7307*	—	—	0
D)											
REC8	1833	16	0.3698	**8**	0	*1.000*	14.690	***0.0006***	5.927	***0.0149***	0
RAD21L	1686	15	0.503	**8**	12.124	***0.0023***	32.050	***>0.0001***	12.049	***0.0005***	**4**
SYCP1	3015	16	0.4337	**8**	8.711	***0.0128***	26.860	***>0.0001***	9.243	***0.0024***	**3**
SYCP2	4650	16	0.5572	**8**	11.584	***0.0031***	37.200	***>0.0001***	15.838	***0.0001***	0
TEX12	369	14	0.2297	7	0.0565	*0.9721*	1.549	*0.4610*	—	—	0
E)											
TEX11	2844	15	0.8483	**8**	60.872	***>0.0001***	82.665	***>0.0001***	61.141	***>0.0001***	**14**
SHOC1	4644	16	0.6113	**8**	12.447	***0.0020***	30.561	***>0.0001***	15.645	***0.0001***	0
RNF212	948	16	0.5014	**8**	0	*1.000*	16.366	***0.0003***	5.202	***0.0226***	**1**
RNF212B	906	14	0.4066	7	0	*1.000*	0.500	*0.7788*	—	—	0

Gene	***bp***	***N***	ω	***M***	***M1-M2***	***p-value***	***M7-M8***	***p-value***	***M8a-M8***	***p-value***	***BEB***
MSH4	2814	16	0.2132	**8**	16.608	***0.0002***	39.447	***>0.0001***	23.238	***>0.0001***	**6**
MSH5	2565	15	0.1642	7	0	*1.000*	4.214	*0.1216*	—	—	0
F)											
MER3	4458	16	0.3633	8a	0	*1.000*	12.838	***0.0016***	3.109	*0.0779*	0
CNTD1	1026	15	0.2496	7	0	*1.000*	0.936	*0.6263*	—	—	0
HEI10	831	15	0.1226	7	0	*1.000*	0.250	*0.8826*	—	—	0
MLH1	2313	15	0.1652	8a	0	*1.000*	12.221	***0.0022***	0.280	*0.5970*	0
MLH3	4419	16	0.4444	7	0	*1.000*	3.757	*0.1528*	—	—	0
MUS81	1665	16	0.2124	7	0	*1.000*	0.628	*0.7304*	—	—	0

Table 4: Evolutionary rates and tests for positive selection across mammals at recombination genes after removal of potential MNMs.

Gene	***bp***	***N***	ω	***M***	***M1-M2***	***p-value***	***M7-M8***	***p-value***	***M8a-M8***	***p-value***
IHO1	1824	16	0.6104	7	0	*1.000*	0.258	*0.8789*	—	—
MRE11	2136	16	0.1330	7	0.226	*0.8930*	3.056	*0.2169*	—	—
NBS1	2289	15	0.3413	7	0	*1.000*	1.956	*0.3761*	—	—
REC8	1833	16	0.2905	7	0	*1.000*	5.321	*0.0699*	—	—
RAD21L	1686	15	0.4271	8a	2.329	*0.3121*	9.497	***0.0087***	1.620	*0.2031*
SYCP1	3015	16	0.3731	8a	3.328	*0.1893*	13.440	***0.0012***	2.122	*0.1452*
SYCP2	4650	16	0.4752	7	0	*1.000*	1.758	*0.4151*	—	—
TEX11	2844	15	0.7287	**8**	9.989	***0.0068***	18.776	***0.0001***	10.656	***0.0011***
SHOC1	4644	16	0.5519	8a	0	*1.000*	7.439	***0.0242***	0.292	*0.5887*
RNF212	948	16	0.3685	7	0	*1.000*	0	*1.000*	—	—
MSH4	2814	16	0.1509	7	0	*1.000*	2.079	*0.3536*	—	—

Table 5: Comparisons of polymorphism within humans to divergence between human and macaque at recombination genes. Genes are organized by step in the pathway, as labeled in Figure 3.

Gene	ω	***Pn***	***Ps***	***Pn/Ps***	***Dn***	***Ds***	***Dn/Ds***	***MK Test***	***NI***	***DoS***	
A)											
HORMAD1	0.0901	43	10	4.3	5	12	0.4167	***0.0002***	10.32	-0.5172	Neg.
MEI4	0.7252	9	2	4.5	24	9	2.6667	*0.7013*	1.6875	-0.0909	—
REC114	0.3239	49	21	2.3333	11	14	0.7857	***0.02949***	2.9700	-0.2600	Neg.
IHO1	0.6608	72	28	2.5714	36	19	1.8947	*0.4658*	1.3571	-0.0645	—
SPO11	0.1434	62	28	2.2143	11	22	0.5000	***0.0008***	4.4286	-0.3556	Neg.
B)											
HORMAD2	0.295	50	16	3.125	7	9	0.7778	***0.0177***	4.0179	-0.3201	Neg.
MRE11	0.0392	139	48	2.8958	5	35	0.1429	***>0.0001***	20.2708	-0.6183	Neg.
NBS1	0.4155	119	58	2.0517	34	25	1.3600	*0.2086*	1.5086	-0.0960	—
RAD50	0.0714	168	55	3.0517	8	43	0.1860	***>0.0001***	16.4182	-0.5965	Neg.
BRCC3	0.0979	7	12	0.5833	2	6	0.3333	*0.6758*	1.7500	-0.1184	—
C)											
DMC1	0.000	43	25	1.72	0	11	0.0000	***<0.0001***	—	-0.6324	Neg.
RAD51	0.000	27	29	0.9310	0	13	0.0000	***0.0010***	—	-0.4821	Neg.
SPATA22	0.4523	67	26	2.5769	21	10	2.1000	*0.6535*	1.2271	-0.0430	—
MEIOB	0.2462	45	17	2.6471	20	22	0.9091	***0.0094***	2.9118	-0.2496	Neg.
MCMDC2	0.2108	90	24	3.7500	16	26	0.6154	***<0.0001***	6.0938	-0.4085	Neg.
D)											
REC8	0.477	90	45	2.000	38	31	1.2258	*0.1264*	1.6316	-0.1159	—
RAD21L	0.6334	21	6	3.500	27	13	2.0769	*0.4176*	1.6852	-0.1028	—
SYCP1	0.3676	122	60	2.033	33	37	1.2222	*0.1204*	1.6636	-0.1203	—
SYCP2	0.3676	246	87	2.8276	74	53	1.3962	***0.0015***	2.0252	-0.1561	Neg.
TEX12	0.1349	15	9	1.6667	2	4	0.5000	*0.3598*	3.3333	-0.2917	—
E)											
TEX11	0.9068	78	45	1.7333	55	25	2.200	*0.4541*	0.7879	0.05335	—
SHOC1	0.7225	227	72	3.1528	85	37	2.2973	*0.2199*	1.3724	-0.0625	—
RNF212	0.387	—	—	—	17	18	0.9444	—	—	—	—
RNF212B	0.2566	9	3	3.000	8	12	0.6667	*0.0759*	4.5000	-0.3500	—

Gene	ω	***Pn***	***Ps***	***Pn/Ps***	***Dn***	***Ds***	***Dn/Ds***	***MK Test***	***NI***	***DoS***	
MSH4	0.2635	149	50	2.9800	24	29	0.8276	***<0.0001***	3.6008	-0.2959	Neg.
MSH5	0.2106	129	64	2.0156	19	33	0.5758	***0.0001***	3.5008	-0.3030	Neg.
F)											
MER3	0.3247	236	92	2.5652	54	44	1.2273	***0.0029***	2.0902	-0.1685	Neg.
CNTD1	0.6803	56	29	1.9310	13	8	1.6250	*0.8001*	1.1883	-0.0398	—
HEI10	0.3235	50	21	2.3810	4	5	0.8000	*0.1417*	2.9762	-0.2598	—
MLH1	0.0924	161	48	3.3542	9	29	0.3103	***>0.0001***	10.8079	-0.5335	Neg.
MLH3	0.4919	252	90	2.8	77	57	1.3509	***0.0009***	2.0727	-0.1622	Neg.
MUS81	0.1299	129	49	2.6327	17	40	0.4250	***>0.0001***	6.1945	-0.4265	Neg.

Supplemental Tables

Table S1: Testes Expression Datasets (Barrett *et al.* 2012)

Species	**GEO Accession**	**Reference**
Bos taurus	GSM1020728 & GSM1020746	Merkin *et al.* (2012)
Callithrix jacchus	GSM1227961, GSM1227962 & GSM1227963	Cortez *et al.* (2014)
Canis lupus familiaris	GSM747469 & GSM1359286	Derti *et al.* (2012), Vandewege *et al.* (2016)
Eptesicus fuscus	GSM1359287	Vandewege *et al.* (2016)
Equus caballus	GSM1139276 & GSM1359288	Coleman *et al.* (2013), Vandewege *et al.* (2016)
Gorilla gorilla	GSM752663	Brawand *et al.* (2011)
Homo sapiens	GSM752707 & GSM752708	Brawand *et al.* (2011)
Macaca mulatta	GSM752642 & GSM752643	Brawand *et al.* (2011)
Mus musculus	GSM752629 & GSM752630	Brawand *et al.* (2011)
Ovis aries	GSM1666944 & GSM1666936	Guan *et al.* (2017)
Pan paniscus	GSM752690	Brawand *et al.* (2011)
Pan troglodytes	GSM752678	Brawand *et al.* (2011)
Pongo pygmaeus	GSM1858310 & GSM1858311	Carelli *et al.* (2016)
Rattus norvegicus	GSM1278058	Cortez *et al.* (2014)
Sus scrofa	GSM1902350, GSM2033157 & GSM2033163	Li *et al.* (2016), Yang *et al.* (2017)
Tupaia chinensis	GSM957062	Fan *et al.* (2013)

455 **Table S2**: NCBI Reference Genomes (O'Leary *et al.* 2015)

Species	**Assembly**	**RefSeq Accession**	**WGS Project Reference**
Bos taurus	Bos_taurus_UMD_3.1.1	GCF_000003055.6	Zimin *et al.* (2009)
Callithrix jacchus	Callithrix_jacchus-3.2	GCF_000004665.1	-
Canis lupus familiaris	CanFam3.1	GCF_000002285.3	Lindblad-Toh *et al.* (2005)
Eptesicus fuscus	EptFus1.0	GCF_000308155.1	-
Equus caballus	EquCab2.0	GCF_000002305.2	Wade *et al.* (2009)
Gorilla gorilla	gorGor4	GCF_000151905.2	Scally *et al.* (2012)
Homo sapiens	GRCh38.p10	GCF_000001405.36	-
Macaca mulatta	Mmul_8.0.1	GCF_000772875.2	Zimin *et al.* (2014)
Mus musculus	GRCm38.p5	GCF_000001635.25	-
Ovis aries	Oar_v4.0	GCF_000298735.2	International Sheep Genomics Consortium *et al.*
Pan paniscus	panpan1.1	GCF_000258655.2	Prüfer *et al.* (2012)
Pan troglodytes	Pan_tro_3.0	GCF_000001515.7	The Chimpanzee Sequencing Analysis Consortiu
Pongo abelii	P_pygmaeus_2.0.2	GCF_000001545.4	Locke *et al.* (2011)
Rattus norvegicus	Rnor_6.0	GCF_000001895.5	Rat Genome Sequencing Project Consortium an
Sus scrofa	Sscrofa11.1	GCF_000003025.6	-
Tupaia chinensis	TupChi_1.0	GCF_000334495.1	Fan *et al.* (2013)

Table S3: Ensembl Reference Genomes (Zerbino *et al.* 2017)

Species	**Assembly**	**RefSeq Accession**	**WGS Project Reference**
Bos taurus	Bos_taurus_UMD_3.1	GCF_000003055.3	Zimin *et al.* (2009)
Callithrix jacchus	Callithrix_jacchus-3.2	GCF_000004665.1	-
Canis lupus familiaris	CanFam3.1	GCF_000002285.3	Lindblad-Toh *et al.* (2005)
Eptesicus fuscus	-	-	-
Equus caballus	EquCab2.0	GCF_000002305.2	Wade *et al.* (2009)
Gorilla gorilla	gorGor3.1	GCF_000151905.1	-
Homo sapiens	GRCh38.p10	GCF_000001405.36	-
Macaca mulatta	Mmul_8.0.1	GCF_000772875.2	Zimin *et al.* (2014)
Mus musculus	GRCm38.p5	GCF_000001635.25	-
Ovis aries	Oar_v3.1	GCF_000298735.1	International Sheep Genomics Consortium *et al.* (
Pan paniscus	panpan1.1	GCF_000258655.2	Prüfer *et al.* (2012)
Pan troglodytes	CHIMP2.1.4	GCF_000001515.6	The Chimpanzee Sequencing Analysis Consortium
Pongo abelii	PPYG2	GCF_000001545.4	Locke *et al.* (2011)
Rattus norvegicus	Rnor_6.0	GCF_000001895.5	Rat Genome Sequencing Project Consortium and
Sus scrofa	Sscrofa11.1	GCF_000003025.6	-
Tupaia chinensis	-	-	-

Table S4: Sequence divergence between human (*Homo sapiens*) and macaque (*Macaca mulatta*) for 32 recombination genes (Yang and Nielsen 2000; Yang 2007).

Gene	***bp***	ω	***S***	***N***	***t***	κ	***dN***	***dS***
A)								
HORMAD1	1182	**0.0901**	273.9	908.1	0.0443	3.8819	0.0044 +- 0.0022	0.0490 +- 0.0137
MEI4	1167	**0.7252**	331	824	0.0822	4.6295	0.0247 +/- 0.0056	0.0341 +/- 0.0104
REC114	864	**0.3239**	237.2	557.8	0.0974	2.9455	0.0200 +/- 0.0061	0.0618 +/- 0.0168
IHO1	1797	**0.6608**	509	1273	0.0951	3.6035	0.0276 +- 0.0047	0.0418 +- 0.0094
SPO11	1188	**0.1434**	291.2	896.8	0.0872	2.5317	0.0118 +/- 0.0036	0.0823 +/- 0.0178
B)								
HORMAD2	921	**0.295**	256.7	664.3	0.0531	4.2164	0.0106 +- 0.0040	0.0360 +- 0.0121
MRE11	2124	**0.0392**	479.4	1644.6	0.0597	2.6154	0.0030 +- 0.0014	0.0778 +- 0.0135
NBS1	2265	**0.4155**	553.7	1705.3	0.0804	5.0955	0.0199 +- 0.0035	0.0480 +- 0.0097
RAD50	3969	**0.0714**	1118.7	2817.3	0.0401	5.0903	0.0028 +- 0.0010	0.0399 +- 0.0062
BRCC3	951	**0.0979**	264	609	0.028	4.6	0.0025 +- 0.0020	0.0252 +- 0.0100
C)								
DMC1	1020	**0.0000**	273.7	746.3	0.0335	5.1279	0.0000 +- 0.0000	0.0416 +- 0.0127
RAD51	1017	**0.0000**	306.5	710.5	0.0398	6.7467	0.0000 +- 0.0000	0.0441 +- 0.0124
SPATA22	1089	**0.4523**	247.8	841.2	0.0879	3.6505	0.0230 +- 0.0053	0.0508 +- 0.0150
MEIOB	1413	**0.2462**	348.9	1064.1	0.0927	4.3887	0.0176 +- 0.0041	0.0715 +- 0.0151
MCMDC2	2043	**0.2108**	534	1509	0.0635	7.8547	0.0107 +- 0.0027	0.0507 +- 0.0101
D)								
REC8	1701	**0.477**	497	1138	0.1293	2.8869	0.0323 +- 0.0054	0.0678 +- 0.0122
RAD21L	1680	**0.6334**	427.5	1237.5	0.0735	5.6876	0.0213 +- 0.0042	0.0337 +- 0.0091
SYCP1	2928	**0.3676**	761.6	2166.4	0.0628	4.8307	0.0145 +- 0.0026	0.0393 +- 0.0074
SYCP2	4590	**0.3873**	1070.7	3519.3	0.0854	5.994	0.0208 +- 0.0025	0.0537 +- 0.0074
TEX12	369	**0.1349**	80.2	288.8	0.05	1.9678	0.0070 +- 0.0049	0.0516 +- 0.0260
E)								
TEX11	2775	**0.9068**	805.9	1933.1	0.0897	7.8022	0.0290 +- 0.0040	0.0320 +- 0.0064
SHOC1	4332	**0.7225**	1203	3129	0.0865	9.5737	0.0261 +- 0.0029	0.0361 +- 0.0057
RNF212	816	**0.387**	243.2	572.8	0.1342	4.996	0.0304 +- 0.0074	0.0785 +- 0.0189
RNF212B	900	**0.2566**	255.6	644.4	0.0685	3.4122	0.0125 +- 0.0044	0.0488 +- 0.0143

Gene	***bp***	ω	***S***	***N***	***t***	κ	***dN***	***dS***
MSH4	2808	**0.2635**	731.3	2073.7	0.058	7.5194	0.0112 +- 0.0023	0.0425 +- 0.0079
MSH5	2502	**0.2106**	728.7	1770.3	0.0643	3.9993	0.0102 +- 0.0024	0.0486 +- 0.0085
F)								
MER3	4305	**0.3247**	987.6	3317.4	0.0703	7.0099	0.0159 +- 0.0022	0.0488 +- 0.0074
CNTD1	990	**0.6803**	335.3	651.7	0.065	8.0721	0.0187 +- 0.0054	0.0274 +- 0.0092
HEI10	1059	**0.3235**	241.5	589.5	0.0329	5.9591	0.0068 +- 0.0034	0.0211 +- 0.0095
MLH1	2268	**0.0924**	602.3	1665.7	0.0522	2.4752	0.0048 +- 0.0017	0.0521 +- 0.0097
MLH3	4368	**0.4919**	1209.8	3149.2	0.0949	6.4296	0.0246 +- 0.0028	0.0500 +- 0.0067
MUS81	1653	**0.1299**	465.8	1187.2	0.1106	5.7915	0.0128 +- 0.0033	0.0983 +- 0.0158

459 **Table S5**: Evolutionary rates and tests for positive selection across mammals at 32 recombination genes
460 using the gene tree. Genes are organized by step in the pathway, as labeled in Figure 3. (Yang 2007).

Gene	***bp***	***N***	ω	***M***	***M1-M2***	***p-value***	***M7-M8***	***p-value***	***M8a-M8***	***p-value***
A)										
HORMAD1	1212	16	0.3037	7	0	*1.000*	3.135	*0.2086*	—	—
MEI4	1170	16	0.4310	7	0	*1.000*	0.058	*0.9715*	—	—
REC114	870	15	0.4237	7	0	*1.000*	4.1874	*0.1232*	—	—
IHO1	1824	16	0.7099	**8**	13.384	***0.0012***	17.714	***0.0001***	14.707	***0.0001***
SPO11	1188	15	0.1701	7	0	*1.000*	4.697	*0.0955*	—	—
B)										
HORMAD2	981	15	0.3290	1	0	*1.000*	3.881	*0.1436*	—	—
MRE11	2136	16	0.1686	**8**	0.636	*0.7277*	12.014	***0.0025***	4.822	***0.0281***
NBS1	2289	15	0.4185	**8**	0	*1.000*	12.899	***0.0016***	4.298	***0.0382***
RAD50	3936	16	0.0322	1	0	*1.000*	0.5615	*0.7552*	—	—-
BRCC3	954	15	0.0601	7	0	*1.000*	0.573	*0.7509*	—	—
C)										
DMC1	1020	15	0.0365	7	0	*1.000*	4.288	*0.1172*	—	—
RAD51	1017	16	0.0322	1	0	*1.000*	0.562	*0.7552*	—	—
SPATA22	1101	16	0.4932	7	0	*1.000*	0.200	*0.9049*	—	—
MEIOB	1425	16	0.2340	7	0	*1.000*	0.221	*0.8955*	—	—
MCMDC2	2052	16	0.2242	7	0	*1.000*	0.610	*0.7370*	—	—
D)										
REC8	1833	16	0.3698	**8**	0	*1.000*	14.690	***0.0006***	5.927	***0.0149***
RAD21L	1686	15	0.503	**8**	12.124	***0.0023***	32.050	***>0.0001***	12.049	***0.0005***
SYCP1	3015	16	0.4337	**8**	8.711	***0.0128***	26.860	***>0.0001***	9.243	***0.0024***
SYCP2	4650	16	0.5572	**8**	11.584	***0.0031***	37.200	***>0.0001***	15.838	***0.0001***
TEX12	369	14	0.2297	7	0.0565	*0.9721*	1.549	*0.4610*	—	—
E)										
TEX11	2844	15	0.8483	**8**	60.872	***>0.0001***	82.665	***>0.0001***	61.141	***>0.0001***
SHOC1	4644	16	0.6113	**8**	12.447	***0.0020***	30.561	***>0.0001***	15.645	***0.0001***
RNF212	948	16	0.5014	**8**	0	*1.000*	16.366	***0.0003***	5.202	***0.0226***
RNF212B	906	14	0.4066	7	0	*1.000*	0.500	*0.7788*	—	—

Gene	***bp***	***N***	ω	***M***	***M1-M2***	***p-value***	***M7-M8***	***p-value***	***M8a-M8***	***p-value***
MSH4	2814	16	0.2132	**8**	16.608	***0.0002***	39.447	***>0.0001***	23.238	***>0.0001***
MSH5	2565	15	0.1642	7	0	*1.000*	4.214	*0.1216*	—	—
F)										
MER3	4458	16	0.3633	8a	0	*1.000*	12.838	***0.0016***	3.109	*0.0779*
CNTD1	1026	15	0.2496	7	0	*1.000*	0.936	*0.6263*	—	—
HEI10	831	15	0.1226	7	0	*1.000*	0.250	*0.8826*	—	—
MLH1	2313	15	0.1652	8a	0	*1.000*	12.221	***0.0022***	0.280	*0.5970*
MLH3	4419	16	0.4444	7	0	*1.000*	3.757	*0.1528*	—	—
MUS81	1665	16	0.2124	7	0	*1.000*	0.628	*0.7304*	—	—

References

Abascal F., R. Zardoya, and M. J. Telford, 2010 TranslatorX: Multiple alignment of nucleotide sequences guided by amino acid translations. Nucleic acids research 38: W7–W13.

Baker S. M., A. W. Plug, T. A. Prolla, C. E. Bronner, and A. C. Harris *et al.*, 1996 Involvement of mouse Mlh1 in DNA mismatch repair and meiotic crossing over. Nature genetics 13: 336.

Balcova M., B. Faltusova, V. Gergelits, T. Bhattacharyya, and O. Mihola *et al.*, 2016 Hybrid sterility locus on chromosome X controls meiotic recombination rate in mouse. PLoS genetics 12: e1005906.

Barbosa-Morais N. L., M. Irimia, Q. Pan, H. Y. Xiong, and S. Gueroussov *et al.*, 2012 The evolutionary landscape of alternative splicing in vertebrate species. Science 338: 1587–1593.

Barrett T., S. E. Wilhite, P. Ledoux, C. Evangelista, and I. F. Kim *et al.*, 2012 NCBI geo: Archive for functional genomics data sets—update. Nucleic acids research 41: D991–D995.

Baudat F., K. Manova, J. P. Yuen, M. Jasin, and S. Keeney, 2000 Chromosome synapsis defects and sexually dimorphic meiotic progression in mice lacking Spo11. Molecular cell 6: 989–998.

Baudat F., and B. de Massy, 2007 Regulating double-stranded dna break repair towards crossover or non-crossover during mammalian meiosis. Chromosome research 15: 565–577.

Begun D. J., and C. F. Aquadro, 1992 Levels of naturally occurring DNA polymorphism correlate with recombination rates in D. Melanogaster. Nature 356: 519.

Bergerat A., B. de Massy, D. Gadelle, P.-C. Varoutas, and A. Nicolas *et al.*, 1997 An atypical topoisomerase II from Archaea with implications for meiotic recombination. Nature 386: 414.

Besenbacher S., P. Sulem, A. Helgason, H. Helgason, and H. Kristjansson *et al.*, 2016 Multi-nucleotide de novo mutations in humans. PLoS genetics 12: e1006315.

Bisig C. G., M. F. Guiraldelli, A. Kouznetsova, H. Scherthan, and C. Höög *et al.*, 2012 Synaptonemal complex components persist at centromeres and are required for homologous centromere pairing in mouse spermatocytes. PLoS genetics 8: e1002701.

Bolcun-Filas E., and J. C. Schimenti, 2012 Genetics of meiosis and recombination in mice. International review of cell and molecular biology 298: 179–227.

Brand C. L., M. V. Cattani, S. B. Kingan, E. L. Landeen, and D. C. Presgraves, 2018 Molecular evolution at a meiosis gene mediates species differences in the rate and patterning of recombination. Current Biology 28:

1289–1295.

Brawand D., M. Soumillon, A. Necsulea, P. Julien, and G. Csárdi *et al.*, 2011 The evolution of gene expression levels in mammalian organs. Nature 478: 343.

Broman K. W., J. C. Murray, V. C. Sheffield, R. L. White, and J. L. Weber, 1998 Comprehensive human genetic maps: Individual and sex-specific variation in recombination. The American Journal of Human Genetics 63: 861–869.

Brown M. S., and D. K. Bishop, 2014 DNA strand exchange and RecA homologs in meiosis. Cold Spring Harbor perspectives in biology a016659.

Burt A., and G. Bell, 1987 Red queen versus tangled bank models. Nature 330: 118.

Carelli F. N., T. Hayakawa, Y. Go, H. Imai, and M. Warnefors *et al.*, 2016 The life history of retrocopies illuminates the evolution of new mammalian genes. Genome research gr–198473.

Charlesworth B., M. Morgan, and D. Charlesworth, 1993 The effect of deleterious mutations on neutral molecular variation. Genetics 134: 1289–1303.

Charlesworth B., 1994 The effect of background selection against deleterious mutations on weakly selected, linked variants. Genetics Research 63: 213–227.

Charlesworth B., P. Jarne, and S. Assimacopoulos, 1994 The distribution of transposable elements within and between chromosomes in a population of drosophila melanogaster. III. Element abundances in heterochromatin. Genetics Research 64: 183–197.

Chen M.-Y., D. Liang, and P. Zhang, 2017 Phylogenomic resolution of the phylogeny of laurasiatherian mammals: Exploring phylogenetic signals within coding and noncoding sequences. Genome biology and evolution 9: 1998–2012.

Chowdhury R., P. R. Bois, E. Feingold, S. L. Sherman, and V. G. Cheung, 2009 Genetic analysis of variation in human meiotic recombination. PLoS genetics 5: e1000648.

Clark N. L., J. Gasper, M. Sekino, S. A. Springer, and C. F. Aquadro *et al.*, 2009 Coevolution of interacting fertilization proteins. PLoS genetics 5: e1000570.

Clark N. L., E. Alani, and C. F. Aquadro, 2012 Evolutionary rate covariation reveals shared functionality and coexpression of genes. Genome research.

Clark N. L., E. Alani, and C. F. Aquadro, 2013 Evolutionary rate covariation in meiotic proteins results from fluctuating evolutionary pressure in yeasts and mammals. Genetics 193: 529–538.

Cloud V., Y.-L. Chan, J. Grubb, B. Budke, and D. K. Bishop, 2012 Rad51 is an accessory factor for Dmc1-mediated joint molecule formation during meiosis. Science 337: 1222–1225.

Coleman S. J., Z. Zeng, M. S. Hestand, J. Liu, and J. N. Macleod, 2013 Analysis of unannotated equine transcripts identified by mRNA sequencing. PLoS One 8: e70125.

Comeron J. M., M. Kreitman, and M. Aguadé, 1999 Natural selection on synonymous sites is correlated with gene length and recombination in drosophila. Genetics 151: 239–249.

Comeron J. M., R. Ratnappan, and S. Bailin, 2012 The many landscapes of recombination in drosophila melanogaster. PLoS genetics 8: e1002905.

Coop G., and M. Przeworski, 2007 An evolutionary view of human recombination. Nature Reviews Genetics 8: 23.

Cortez D., R. Marin, D. Toledo-Flores, L. Froidevaux, and A. Liechti *et al.*, 2014 Origins and functional evolution of Y chromosomes across mammals. Nature 508: 488.

Costa Y., R. Speed, R. Öllinger, M. Alsheimer, and C. A. Semple *et al.*, 2005 Two novel proteins recruited by synaptonemal complex protein 1 (SYCP1) are at the centre of meiosis. Journal of cell science 118: 2755–2762.

Dapper A. L., and M. J. Wade, 2016 The evolution of sperm competition genes: The effect of mating system on levels of genetic variation within and between species. Evolution 70: 502–511.

Dapper A. L., and B. A. Payseur, 2017 Connecting theory and data to understand recombination rate evolution. Phil. Trans. R. Soc. B 372: 20160469.

Derti A., P. Garrett-Engele, K. D. MacIsaac, R. C. Stevens, and S. Sriram *et al.*, 2012 A quantitative atlas of polyadenylation in five mammals. Genome research gr–132563.

Dong Y., M.-A. Hakimi, X. Chen, E. Kumaraswamy, and N. S. Cooch *et al.*, 2003 Regulation of BRCC, a holoenzyme complex containing BRCA1 and BRCA2, by a signalosome-like subunit and its role in dna repair. Molecular cell 12: 1087–1099.

Dumont B. L., and B. A. Payseur, 2008 Evolution of the genomic rate of recombination in mammals. Evolution: International Journal of Organic Evolution 62: 276–294.

Dumont B. L., and B. A. Payseur, 2011 Genetic analysis of genome-scale recombination rate evolution in house mice. PLoS genetics 7: e1002116.

Dumont B. L., M. A. White, B. Steffy, T. Wiltshire, and B. A. Payseur, 2011 Extensive recombination rate variation in the house mouse species complex inferred from genetic linkage maps. Genome research 21:

114–125.

Duret L., and D. Mouchiroud, 1999 Expression pattern and, surprisingly, gene length shape codon usage in Caenorhabditis, Drosophila, and Arabidopsis. Proceedings of the National Academy of Sciences 96: 4482–4487.

Duret L., and P. F. Arndt, 2008 The impact of recombination on nucleotide substitutions in the human genome. PLoS genetics 4: e1000071.

Edelmann W., P. E. Cohen, M. Kane, K. Lau, and B. Morrow *et al.*, 1996 Meiotic pachytene arrest in MLH1-deficient mice. Cell 85: 1125–1134.

Edgar R. C., 2004 MUSCLE: Multiple sequence alignment with high accuracy and high throughput. Nucleic acids research 32: 1792–1797.

Fan Y., Z.-Y. Huang, C.-C. Cao, C.-S. Chen, and Y.-X. Chen *et al.*, 2013 Genome of the Chinese tree shrew. Nature communications 4: 1426.

Fay J. C., G. J. Wyckoff, and C.-I. Wu, 2001 Positive and negative selection on the human genome. Genetics 158: 1227–1234.

Felsenstein J., 1974 The evolutionary advantage of recombination. Genetics 78: 737–756.

Finsterbusch F., R. Ravindranathan, I. Dereli, M. Stanzione, and D. Tränkner *et al.*, 2016 Alignment of homologous chromosomes and effective repair of programmed dna double-strand breaks during mouse meiosis require the minichromosome maintenance domain containing 2 (MCMDC2) protein. PLoS genetics 12: e1006393.

Fledel-Alon A., E. M. Leffler, Y. Guan, M. Stephens, and G. Coop *et al.*, 2011 Variation in human recombination rates and its genetic determinants. PloS one 6: e20321.

Fraune J., M. Alsheimer, J. Redolfi, C. Brochier-Armanet, and R. Benavente, 2014 Protein SYCP2 is an ancient component of the metazoan synaptonemal complex. Cytogenetic and genome research 144: 299–305.

Gonen S., M. Battagin, S. E. Johnston, G. Gorjanc, and J. M. Hickey, 2017 The potential of shifting recombination hotspots to increase genetic gain in livestock breeding. Genetics Selection Evolution 49: 55.

Grey C., P. Barthès, Chauveau-Le FriecG., F. Langa, and F. Baudat *et al.*, 2011 Mouse PRDM9 DNA-binding specificity determines sites of histone H3 lysine 4 trimethylation for initiation of meiotic recombination. PLoS biology 9: e1001176.

Grey C., F. Baudat, and B. de Massy, 2018 PRDM9, a driver of the genetic map. PLoS genetics 14: e1007479.

Guan Y., G. Liang, G. B. Martin, and others, 2017 Functional changes in mRNA expression and alternative pre-mRNA splicing associated with the effects of nutrition on apoptosis and spermatogenesis in the adult testis. BMC genomics 18: 64.

Guiraldelli M. F., A. Felberg, L. P. Almeida, A. Parikh, and R. O. de Castro *et al.*, 2018 SHOC1 is a ERCC4-(HhH) 2-like protein, integral to the formation of crossover recombination intermediates during mammalian meiosis. PLoS genetics 14: e1007381.

Hakes L., S. C. Lovell, S. G. Oliver, and D. L. Robertson, 2007 Specificity in protein interactions and its relationship with sequence diversity and coevolution. Proceedings of the National Academy of Sciences 104: 7999–8004.

Hamer G., K. Gell, A. Kouznetsova, I. Novak, and R. Benavente *et al.*, 2006 Characterization of a novel meiosis-specific protein within the central element of the synaptonemal complex. Journal of cell science 119: 4025–4032.

Hamer G., H. Wang, E. Bolcun-Filas, H. J. Cooke, and R. Benavente *et al.*, 2008 Progression of meiotic recombination requires structural maturation of the central element of the synaptonemal complex. Journal of cell science 121: 2445–2451.

Hassold T., and P. Hunt, 2001 To err (meiotically) is human: The genesis of human aneuploidy. Nature Reviews Genetics 2: 280.

Hernández-Hernández A., S. Masich, T. Fukuda, A. Kouznetsova, and S. Sandin *et al.*, 2016 The central element of the synaptonemal complex in mice is organized as a bilayered junction structure. J Cell Sci 129: 2239–2249.

Hill W. G., and A. Robertson, 1966 The effect of linkage on limits to artificial selection. Genetics Research 8: 269–294.

Hopfner K.-P., 2005 Structure and function of Rad50/SMC protein complexes in chromosome biology, pp. 201–218 in *Genome integrity*, Springer.

Hunter C. M., W. Huang, T. F. Mackay, and N. D. Singh, 2016 The genetic architecture of natural variation in recombination rate in drosophila melanogaster. PLoS genetics 12: e1005951.

International Sheep Genomics Consortium, A. Archibald, N. Cockett, B. Dalrymple, and T. Faraut *et al.*, 2010 The sheep genome reference sequence: A work in progress. Animal genetics 41: 449–453.

Jeffreys A. J., R. Neumann, M. Panayi, S. Myers, and P. Donnelly, 2005 Human recombination hot spots

hidden in regions of strong marker association. Nature genetics 37: 601.

Johnston S. E., C. Bérénos, J. Slate, and J. M. Pemberton, 2016 Conserved genetic architecture underlying individual recombination rate variation in a wild population of Soay sheep (Ovis aries). Genetics genetics–115.

Johnston S. E., J. Huisman, and J. M. Pemberton, 2018 A genomic region containing REC8 and RNF212B is associated with individual recombination rate variation in a wild population of red deer (Cervus elaphus). G3: Genes, Genomes, Genetics g3–200063.

Kadri N. K., C. Harland, P. Faux, N. Cambisano, and L. Karim *et al.*, 2016 Coding and noncoding variants in HFM1, MLH3, MSH4, MSH5, RNF212, and RNF212B affect recombination rate in cattle. Genome research.

Keeney S., C. N. Giroux, and N. Kleckner, 1997 Meiosis-specific DNA double-strand breaks are catalyzed by Spo11, a member of a widely conserved protein family. Cell 88: 375–384.

Keeney S., 2007 Spo11 and the formation of DNA double-strand breaks in meiosis, pp. 81–123 in *Recombination and meiosis*, Springer.

Kobayashi W., M. Takaku, S. Machida, H. Tachiwana, and K. Maehara *et al.*, 2016 Chromatin architecture may dictate the target site for DMC1, but not for RAD51, during homologous pairing. Scientific reports 6: 24228.

Kohl K. P., C. D. Jones, and J. Sekelsky, 2012 Evolution of an MCM complex in flies that promotes meiotic crossovers by blocking BLM helicase. Science 338: 1363–1365.

Kong A., G. Thorleifsson, H. Stefansson, G. Masson, and A. Helgason *et al.*, 2008 Sequence variants in the RNF212 gene associate with genome-wide recombination rate. Science 319: 1398–1401.

Kong A., G. Thorleifsson, D. F. Gudbjartsson, G. Masson, and A. Sigurdsson *et al.*, 2010 Fine-scale recombination rate differences between sexes, populations and individuals. Nature 467: 1099.

Kong A., G. Thorleifsson, M. L. Frigge, G. Masson, and D. F. Gudbjartsson *et al.*, 2014 Common and low-frequency variants associated with genome-wide recombination rate. Nature genetics 46: 11.

Kumar R., N. Ghyselinck, K.-i. Ishiguro, Y. Watanabe, and A. Kouznetsova *et al.*, 2015 MEI4: A central player in the regulation of meiotic dna double strand break formation in the mouse. J Cell Sci jcs–165464.

Lange J., S. Yamada, S. E. Tischfield, J. Pan, and S. Kim *et al.*, 2016 The landscape of mouse meiotic double-strand break formation, processing, and repair. Cell 167: 695–708.

Langmead B., and S. L. Salzberg, 2012 Fast gapped-read alignment with Bowtie 2. Nature methods 9: 357.

La Salle S., K. Palmer, O'BrienM., J. C. Schimenti, and J. Eppig *et al.*, 2012 Spata22, a novel vertebrate-specific gene, is required for meiotic progress in mouse germ cells. Biology of reproduction 86: 45–1.

Latrille T., L. Duret, and N. Lartillot, 2017 The red queen model of recombination hot-spot evolution: A theoretical investigation. Phil. Trans. R. Soc. B 372: 20160463.

Lee J., and T. Hirano, 2011 RAD21L, a novel cohesin subunit implicated in linking homologous chromosomes in mammalian meiosis. The Journal of cell biology 192: 263–276.

Leinonen R., H. Sugawara, M. Shumway, and I. N. S. D. Collaboration, 2010 The sequence read archive. Nucleic acids research 39: D19–D21.

Lek M., K. J. Karczewski, E. V. Minikel, K. E. Samocha, and E. Banks *et al.*, 2016 Analysis of protein-coding genetic variation in 60,706 humans. Nature 536: 285.

Lesecque Y., S. Glémin, N. Lartillot, D. Mouchiroud, and L. Duret, 2014 The red queen model of recombination hotspots evolution in the light of archaic and modern human genomes. PLoS genetics 10: e1004790.

Li H., B. Handsaker, A. Wysoker, T. Fennell, and J. Ruan *et al.*, 2009 The sequence alignment/map format and samtools. Bioinformatics 25: 2078–2079.

Li Y., J. Li, C. Fang, L. Shi, and J. Tan *et al.*, 2016 Genome-wide differential expression of genes and small rnas in testis of two different porcine breeds and at two different ages. Scientific reports 6: 26852.

Liao B.-Y., N. M. Scott, and J. Zhang, 2006 Impacts of gene essentiality, expression pattern, and gene compactness on the evolutionary rate of mammalian proteins. Molecular biology and evolution 23: 2072–2080.

Lindblad-Toh K., C. M. Wade, T. S. Mikkelsen, E. K. Karlsson, and D. B. Jaffe *et al.*, 2005 Genome sequence, comparative analysis and haplotype structure of the domestic dog. Nature 438: 803.

Lipkin S. M., P. B. Moens, V. Wang, M. Lenzi, and D. Shanmugarajah *et al.*, 2002 Meiotic arrest and aneuploidy in MLH3-deficient mice. Nature genetics 31: 385.

Locke D. P., L. W. Hillier, W. C. Warren, K. C. Worley, and L. V. Nazareth *et al.*, 2011 Comparative and demographic analysis of orang-utan genomes. Nature 469: 529.

Lu Y., and M. D. Rausher, 2003 Evolutionary rate variation in anthocyanin pathway genes. Molecular biology and evolution 20: 1844–1853.

Ma L., O'ConnellJ. R., P. M. VanRaden, B. Shen, and A. Padhi *et al.*, 2015 Cattle sex-specific recombination and genetic control from a large pedigree analysis. PLoS genetics 11: e1005387.

McDonald J. H., and M. Kreitman, 1991 Adaptive protein evolution at the Adh locus in Drosophila. Nature 351: 652.

Merkin J., C. Russell, P. Chen, and C. B. Burge, 2012 Evolutionary dynamics of gene and isoform regulation in mammalian tissues. Science 338: 1593–1599.

Meuwissen R., H. H. Offenberg, A. Dietrich, A. Riesewijk, and M. van Iersel *et al.*, 1992 A coiled-coil related protein specific for synapsed regions of meiotic prophase chromosomes. The EMBO Journal 11: 5091.

Murdoch B., N. Owen, S. Shirley, S. Crumb, and K. W. Broman *et al.*, 2010 Multiple loci contribute to genome-wide recombination levels in male mice. Mammalian genome 21: 550–555.

Myers S., R. Bowden, A. Tumian, R. E. Bontrop, and C. Freeman *et al.*, 2010 Drive against hotspot motifs in primates implicates the prdm9 gene in meiotic recombination. Science 327: 876–879.

Oh J., A. Al-Zain, E. Cannavo, P. Cejka, and L. S. Symington, 2016 Xrs2 dependent and independent functions of the Mre11-Rad50 complex. Molecular cell 64: 405–415.

O'Leary N. A., M. W. Wright, J. R. Brister, S. Ciufo, and D. Haddad *et al.*, 2015 Reference sequence (RefSeq) database at NCBI: Current status, taxonomic expansion, and functional annotation. Nucleic acids research 44: D733–D745.

Oliver P. L., L. Goodstadt, J. J. Bayes, Z. Birtle, and K. C. Roach *et al.*, 2009 Accelerated evolution of the Prdm9 speciation gene across diverse metazoan taxa. PLoS genetics 5: e1000753.

Page S. L., and R. S. Hawley, 2004 The genetics and molecular biology of the synaptonemal complex. Annu. Rev. Cell Dev. Biol. 20: 525–558.

Pamilo P., and M. Nei, 1988 Relationships between gene trees and species trees. Molecular biology and evolution 5: 568–583.

Pan Q., O. Shai, L. J. Lee, B. J. Frey, and B. J. Blencowe, 2008 Deep surveying of alternative splicing complexity in the human transcriptome by high-throughput sequencing. Nature genetics 40: 1413.

Parisi S., M. J. McKay, M. Molnar, M. A. Thompson, and Van Der SpekP. J. *et al.*, 1999 Rec8p, a meiotic recombination and sister chromatid cohesion phosphoprotein of the Rad21p family conserved from fission yeast to humans. Molecular and cellular biology 19: 3515–3528.

Parvanov E. D., P. M. Petkov, and K. Paigen, 2010 Prdm9 controls activation of mammalian recombination hotspots. Science 327: 835–835.

689 Pazos F., and A. Valencia, 2001 Similarity of phylogenetic trees as indicator of protein–protein interaction.
690 Protein engineering 14: 609–614.

691 Perelman P., W. E. Johnson, C. Roos, H. N. Seuánez, and J. E. Horvath *et al.*, 2011 A molecular phylogeny
692 of living primates. PLoS genetics 7: e1001342.

693 Petit M., J.-M. Astruc, J. Sarry, L. Drouilhet, and S. Fabre *et al.*, 2017 Variation in recombination rate and
694 its genetic determinism in sheep populations. Genetics genetics–300123.

695 Piovesan D., F. Tabaro, L. Paladin, M. Necci, and I. Mičetić *et al.*, 2017 MobiDB 3.0: More annotations for
696 intrinsic disorder, conformational diversity and interactions in proteins. Nucleic acids research 46: D471–D476.

697 Prasad A. B., M. W. Allard, N. C. S. Program, and E. D. Green, 2008 Confirming the phylogeny of mammals
698 by use of large comparative sequence data sets. Molecular Biology and Evolution 25: 1795–1808.

699 Priedigkeit N., N. Wolfe, and N. L. Clark, 2015 Evolutionary signatures amongst disease genes permit novel
700 methods for gene prioritization and construction of informative gene-based networks. PLoS genetics 11:
701 e1004967.

702 Prüfer K., K. Munch, I. Hellmann, K. Akagi, and J. R. Miller *et al.*, 2012 The bonobo genome compared
703 with the chimpanzee and human genomes. Nature 486: 527.

704 Qiao H., H. P. Rao, Y. Yang, J. H. Fong, and J. M. Cloutier *et al.*, 2014 Antagonistic roles of ubiquitin ligase
705 HEI10 and SUMO ligase RNF212 regulate meiotic recombination. Nature genetics 46: 194.

706 Rakshambikai R., N. Srinivasan, and K. T. Nishant, 2013 Structural insights into saccharomyces cerevisiae
707 Msh4–Msh5 complex function using homology modeling. PLoS One 8: e78753.

708 Rao H. P., H. Qiao, S. K. Bhatt, L. R. Bailey, and H. D. Tran *et al.*, 2017 A sumo-ubiquitin relay recruits
709 proteasomes to chromosome axes to regulate meiotic recombination. Science 355: 403–407.

710 Rat Genome Sequencing Project Consortium, and others, 2004 Genome sequence of the brown norway rat
711 yields insights into mammalian evolution. Nature 428: 493.

712 Rausher M. D., R. E. Miller, and P. Tiffin, 1999 Patterns of evolutionary rate variation among genes of the
713 anthocyanin biosynthetic pathway. Molecular biology and evolution 16: 266–274.

714 R Core Team, 2015 R: A language and environment for statistical computing

715 Reynolds A., H. Qiao, Y. Yang, J. K. Chen, and N. Jackson *et al.*, 2013 RNF212 is a dosage-sensitive regulator
716 of crossing-over during mammalian meiosis. Nature genetics 45: 269.

Ritz K. R., M. A. Noor, and N. D. Singh, 2017 Variation in recombination rate: Adaptive or not? Trends in Genetics 33: 364–374.

Rogacheva M. V., C. M. Manhart, C. Chen, A. Guarne, and J. Surtees *et al.*, 2014 Mlh1-Mlh3, a meiotic crossover and DNA mismatch repair factor, is a Msh2-Msh3-stimulated endonuclease. Journal of Biological Chemistry jbc–M113.

Romanienko P. J., and R. D. Camerini-Otero, 2000 The mouse Spo11 gene is required for meiotic chromosome synapsis. Molecular cell 6: 975–987.

Ronquist F., M. Teslenko, Van Der MarkP., D. L. Ayres, and A. Darling *et al.*, 2012 MrBayes 3.2: Efficient Bayesian phylogenetic inference and model choice across a large model space. Systematic biology 61: 539–542.

Rosenberg N. A., 2002 The probability of topological concordance of gene trees and species trees. Theoretical population biology 61: 225–247.

Sandor C., W. Li, W. Coppieters, T. Druet, and C. Charlier *et al.*, 2012 Genetic variants in REC8, RNF212, and PRDM9 influence male recombination in cattle. PLoS genetics 8: e1002854.

Scally A., J. Y. Dutheil, L. W. Hillier, G. E. Jordan, and I. Goodhead *et al.*, 2012 Insights into hominid evolution from the gorilla genome sequence. Nature 483: 169.

Schmekel K., and B. Daneholt, 1995 The central region of the synaptonemal complex revealed in three dimensions. Trends in cell biology 5: 239–242.

Schramm S., J. Fraune, R. Naumann, A. Hernandez-Hernandez, and C. Höög *et al.*, 2011 A novel mouse synaptonemal complex protein is essential for loading of central element proteins, recombination, and fertility. PLoS genetics 7: e1002088.

Schrider D. R., J. N. Hourmozdi, and M. W. Hahn, 2011 Pervasive multinucleotide mutational events in eukaryotes. Current Biology 21: 1051–1054.

Scornavacca C., and N. Galtier, 2017 Incomplete lineage sorting in mammalian phylogenomics. Systematic biology 66: 112–120.

Segura J., L. Ferretti, S. Ramos-Onsins, L. Capilla, and M. Farré *et al.*, 2013 Evolution of recombination in eutherian mammals: Insights into mechanisms that affect recombination rates and crossover interference. Proceedings of the Royal Society of London B: Biological Sciences 280: 20131945.

Shen B., J. Jiang, E. Seroussi, G. E. Liu, and L. Ma, 2018 Characterization of recombination features and the genetic basis in multiple cattle breeds. BMC genomics 19: 304.

Smith N. G., and A. Eyre-Walker, 2002 Adaptive protein evolution in Drosophila. Nature 415: 1022.

Smukowski C., and M. Noor, 2011 Recombination rate variation in closely related species. Heredity 107: 496.

Snowden T., S. Acharya, C. Butz, M. Berardini, and R. Fishel, 2004 hMSH4-hMSH5 recognizes Holliday junctions and forms a meiosis-specific sliding clamp that embraces homologous chromosomes. Molecular cell 15: 437–451.

Stanzione M., M. Baumann, F. Papanikos, I. Dereli, and J. Lange *et al.*, 2016 Meiotic DNA break formation requires the unsynapsed chromosome axis-binding protein IHO1 (CCDC36) in mice. Nature cell biology 18: 1208.

Stapley J., P. G. Feulner, S. E. Johnston, A. W. Santure, and C. M. Smadja, 2017 Variation in recombination frequency and distribution across eukaryotes: Patterns and processes. Phil. Trans. R. Soc. B 372: 20160455.

Stoletzki N., and A. Eyre-Walker, 2010 Estimation of the neutrality index. Molecular biology and evolution 28: 63–70.

Swanson W. J., and V. D. Vacquier, 2002 The rapid evolution of reproductive proteins. Nature reviews genetics 3: 137.

Swanson W. J., R. Nielsen, and Q. Yang, 2003 Pervasive adaptive evolution in mammalian fertilization proteins. Molecular biology and evolution 20: 18–20.

The Chimpanzee Sequencing Analysis Consortium, R. H. Waterson, E. S. Lander, and R. K. Wilson, 2005 Initial sequence of the chimpanzee genome and comparison with the human genome. Nature 437: 69.

Thomas J. H., R. O. Emerson, and J. Shendure, 2009 Extraordinary molecular evolution in the PRDM9 fertility gene. PloS one 4: e8505.

Thorvaldsdóttir H., J. T. Robinson, and J. P. Mesirov, 2013 Integrative Genomics Viewer (IGV): High-performance genomics data visualization and exploration. Briefings in bioinformatics 14: 178–192.

Trapnell C., L. Pachter, and S. L. Salzberg, 2009 TopHat: Discovering splice junctions with RNA-Seq. Bioinformatics 25: 1105–1111.

Ubeda F., and J. Wilkins, 2011 The red queen theory of recombination hotspots. Journal of evolutionary biology 24: 541–553.

Vandewege M. W., R. N. Platt, D. A. Ray, and F. G. Hoffmann, 2016 Transposable element targeting by piRNAs in Laurasiatherians with distinct transposable element histories. Genome biology and evolution 8: 1327–1337.

775 Venkat A., M. W. Hahn, and J. W. Thornton, 2018 Multinucleotide mutations cause false inferences of
776 lineage-specific positive selection. Nature ecology & evolution 2: 1280.

777 Vries S. S. de, E. B. Baart, M. Dekker, A. Siezen, and D. G. de Rooij *et al.*, 1999 Mouse MutS-like protein
778 Msh5 is required for proper chromosome synapsis in male and female meiosis. Genes & Development 13:
779 523–531.

780 Vries F. A. de, E. de Boer, M. van den Bosch, W. M. Baarends, and M. Ooms *et al.*, 2005 Mouse sycp1
781 functions in synaptonemal complex assembly, meiotic recombination, and xy body formation. Genes &
782 development 19: 1376–1389.

783 Wade C., E. Giulotto, S. Sigurdsson, M. Zoli, and S. Gnerre *et al.*, 2009 Genome sequence, comparative
784 analysis, and population genetics of the domestic horse. Science 326: 865–867.

785 Ward J. O., L. G. Reinholdt, W. W. Motley, L. M. Niswander, and D. C. Deacon *et al.*, 2007 Mutation in
786 mouse hei10, an e3 ubiquitin ligase, disrupts meiotic crossing over. PLoS genetics 3: e139.

787 Wheeler D. L., T. Barrett, D. A. Benson, S. H. Bryant, and K. Canese *et al.*, 2006 Database resources of the
788 national center for biotechnology information. Nucleic acids research 35: D5–D12.

789 Xu Y., R. A. Greenberg, E. Schonbrunn, and P. J. Wang, 2017 Meiosis-specific proteins MEIOB and SPATA22
790 cooperatively associate with the single-stranded DNA-binding replication protein A complex and DNA
791 double-strand breaks. Biology of reproduction 96: 1096–1104.

792 Yang Z., 1997 PAML: A program package for phylogenetic analysis by maximum likelihood. Bioinformatics
793 13: 555–556.

794 Yang Z., and R. Nielsen, 2000 Estimating synonymous and nonsynonymous substitution rates under realistic
795 evolutionary models. Molecular Biology and Evolution 17: 32–43.

796 Yang F., De La FuenteR., N. A. Leu, C. Baumann, and K. J. McLaughlin *et al.*, 2006 Mouse SYCP2 is
797 required for synaptonemal complex assembly and chromosomal synapsis during male meiosis. The Journal of
798 Cell Biology 173: 497–507.

799 Yang Z., 2007 PAML 4: Phylogenetic analysis by maximum likelihood. Molecular Biology and Evolution 24:
800 1586–1591. https://doi.org/10.1093/molbev/msm088

801 Yang F., K. Gell, Van Der HeijdenG. W., S. Eckardt, and N. A. Leu *et al.*, 2008 Meiotic failure in male mice
802 lacking an X-linked factor. Genes & development 22: 682–691.

803 Yang F., S. Silber, N. A. Leu, R. D. Oates, and J. D. Marszalek *et al.*, 2015 TEX11 is mutated in infertile

804 men with azoospermia and regulates genome-wide recombination rates in mouse. EMBO molecular medicine
805 7: 1198–1210.

806 Yang Y., G. Liang, G. Niu, Y. Zhang, and R. Zhou *et al.*, 2017 Comparative analysis of dna methylome and
807 transcriptome of skeletal muscle in lean-, obese-, and mini-type pigs. Scientific reports 7: 39883.

808 Zerbino D. R., P. Achuthan, W. Akanni, M. R. Amode, and D. Barrell *et al.*, 2017 Ensembl 2018. Nucleic
809 acids research 46: D754–D761.

810 Zimin A. V., A. L. Delcher, L. Florea, D. R. Kelley, and M. C. Schatz *et al.*, 2009 A whole-genome assembly
811 of the domestic cow, Bos taurus. Genome biology 10: R42.

812 Zimin A. V., A. S. Cornish, M. D. Maudhoo, R. M. Gibbs, and X. Zhang *et al.*, 2014 A new rhesus macaque
813 assembly and annotation for next-generation sequencing analyses. Biology direct 9: 20.